cancer, or multiple myeloma (MM) and their related bone fractures. It has also been observed in patients with rheumatoid arthritis and in menopausal women with osteoporosis. These patients experienced reduced bone mass and extended bone destruction.[7–10] Thus, it is important to understand the mechanism by which human osteoblastic bone formation and osteoclastic bone resorption control the bone mass in these patients so that skeletal-related events (SREs) can be reduced and the quality of life of these patients can be improved.

CD26 is a 110-kDa cell surface glycoprotein with dipeptidyl peptidase IV (DPPIV) activity, which exhibits diverse functional properties.[11–23] It is composed of the following 3 regions: a 6-amino acid cytoplasmic region; a 22-residue hydrophobic transmembrane region; and an extracellular region (Fig. 4*A*). The extracellular region contains a membrane-proximal glycosylated domain, a cysteine-rich domain, and a 260-amino acid COOH-terminal domain with DPPIV enzymatic activity, and it regulates several crucial cytokines and chemokines and especially the signaling pathway related to T-cell activation.[11–13] Our previous studies suggested that CD26 also plays a significant role in tumor pathogenesis and progression. We showed that the epitope recognized by humanized anti-CD26 monoclonal antibody (huCD26mAb) is located at the cell membrane-proximal glycosylated region comprising 247th –340th amino acid regions of human CD26, near the ADA binding domain.[11,12] We also showed that huCD26mAb impairs the growth of CD26-positive mesothelioma.[13] The growth of malignancies such as CD26-positive malignant lymphoma or renal cell carcinoma is also inhibited by anti-CD26m Ab.[14–17] In several tumors, CD26 expression has been found to be associated with a high level of clinical aggressiveness or responsiveness to therapy.[18–20] Moreover, the association of CD26 expression with distant metastases has been reported.[19–21]

Although CD26 is widely expressed in normal cells, including lymphocytes, endothelial cells and epithelial cells, its expression in OCs has not been studied. We have detected the expression of CD26 on multinucleated giant cells in osteolytic bone lesions following metastasis of several malignant tumors. Therefore, we identified that CD26-stained multinucleated cells were OCs but not megakaryocytes. In this study, we demonstrate that CD26 is expressed in normal human OCs and is intensely expressed in activated human OCs with osteolytic bone lesions by metastasis, including multiple myeloma (MM), adenocarcinoma, and their related bone fractures. We here also examine the novel role of CD26 in the function of OCs during human OC development and, using an *in vitro* model for OC differentation, show that the blockade of CD26 by huCD26mAb results in morphological and functional defects in human OCs. In addition, we also define the molecular targets of the CD26 cascade of RANK signaling in human OC development, for the purpose of developing a promising therapy to treat osteolytic bone loss and reduce total SREs.

Materials and Methods

Bone marrow tissue specimens

Collection of human bone marrow specimens from autopsies were generously permitted by the bereaved families. This study was approved by the Ethical Committee at Keio University School of Medicine (permission ID number 2013-0034). The purpose of the study was explained to all bereaved families of patients and their written, informed consent was obtained. The specimens were subjected to immunohistochemical or enzyme-histochemical staining, as described below.

Reagents and cells

Humanized anti-CD26 monoclonal antibody (IgG_1 isotype), huCD26mAb was generously provided by Y's Therapeutics (Tokyo, Japan). The huCD26mAb employed in this study was generated by utilizing the complementarity determining regions of murine anti-human CD26mAb, 14D10, which has no cross-reactivity to murine CD26. Human IgG_1 (Sigma Aldrich, St. Louis, MO, USA) was used as a control. A specific inhibitor against p38 MAPK, SB203580 was purchased from Cell Signaling Technology (Danvers, MA, USA) and an inhibitor against DPPIV, Vildagliptin (Equa) was purchased from Novartis Pharma (Basel, BL, Switzerland). Cytokines, including recombinant human M-CSF and recombinant human sRANKL were purchased from Peprotec (Rockyhill, NJ, USA). Human bone marrow mononuclear cells (BM-MNCs) were purchased from Lonza (Walkersville, MD, USA).

huCD26mAb-F(ab′)$_2$generation and purification

huCD26mAb-F(ab′)$_2$ was generated from huCD26mAb IgG using a Thermo Scientific Pierce F(ab′)$_2$ Preparation Kit (thermo Scientific, Rockford, IL, USA), according to manufacturer's instructions.

Immunohistochemistry and enzyme-histochemistry

Human bone marrow tissue sections were fixed in 10% neutral buffered formalin, embedded in paraffin and sectioned to a thickness of 5μm. These sections were deparaffinized by four rinses with xylene, then rehydrated with a graded series of ethanol solutions. For histology, sections were stained with hematoxylin and eosin. For immunohistochemistry, sections were washed in phosphate-buffered saline (PBS), subjected to antigen retrieval for CD26 staining by autoclave at 120°C for 20 min in 0.01 M sodium citrate (pH 6.0), and exposed to 0.3% H_2O_2 for 10 min to inactivate endogenous peroxidase. The tissue sections were then incubated with the following primary antibodies: goat anti-human CD26 polyclonal antibody (R&D Systems, Minneapolis, MN, USA), Calcitonin receptor antibody (Santa Cruz), Vitronectin receptor antibody (Abcam), or TRAP antibody (Biolegend), at room temperature for 2 hours (CD26) or 1 hour (Calcitonin receptor antibody, Vitronectin receptor antibody, and TRAP antibody) in a humidified chamber. The reaction was visualized using a peroxidase substrate VECTOR SG Kit (Vector Laboratories, Burlingame, CA, USA) or 3, 3′-diaminobenzidine (DAB) (Dojindo Laboratories, Kumamoto, Japan), and the tissue sections were counterstained for nucleus with hematoxylin. TRAP enzyme histochemistry was also performed by staining the bone marrow sections for TRAP activity using 0.5M L (+) tartrate acid, 2.0 M sodium acetate trihydrate and a Histofine Simple Stain Kit (Nichirei Biosciences, Tokyo, Japan), as described and modified.

Osteoclast culture

Human BM-MNCs (1×10^6 cells/well) were cultured with human M-CSF (25 ng/ml; from day 0) plus recombinant soluble RANKL [receptor activator of nuclear factor kappa B (NF-κB) ligand] (50 ng/ml; from day 3) in α-minimum essential medium (α-MEM) (Life Technologies) supplemented with 10% fetal bovine serum (FBS) (Life Technologies), 100 units/ml penicillin and 100 μg/ml streptomycin, in 24-well plates precoated with type I collagen under 5% CO_2 at 37°C. The cells were cultured in the absence or

presence of huCD26mAb, (0.1, 1.0, 10 μg/ml) or SB203580 (0, 10, 20, or 100 μM). OC precursor cells were grown with M-CSF (25 ng/ml) from day 0 for 3 days, then sRANKL was added at 50 ng/ml from day 3 for the time durations indicated. Culture media with cytokine supplementation were changed every 2 days. Human OCs identified as TRAP-expressing multinuclear giant cells (nuclei > 3) were formed within 7 days. Cultured cells were washed with PBS 3 times, fixed with 4% paraformaldehyde (PFA) for 15 min, and then stained for TRAP activity using a Histofine Simple Stain Kit (Nichirei Biosciences), as described and modified. Red-stained OCs were viewed with an Olympus IX70 microscope (original magnification: ×100, ×200), and images were taken with an Olympus DP21 camera and processed. The number of TRAP-positive OCs and the number of nuclei within the OCs were counted in 10 random fields of view. Three independent experiments were performed using cells from three different donors.

huCD26mAb protocol of *in vitro* human osteoclast (OC) development

Human OC culture was performed in the absence or presence of huCD26mAb (0, 0.1, 1.0, 10 μg/ml). huCD26mAb was added every 48 hours, for a total of 4 doses from day 0 (on day 0, 2, 4

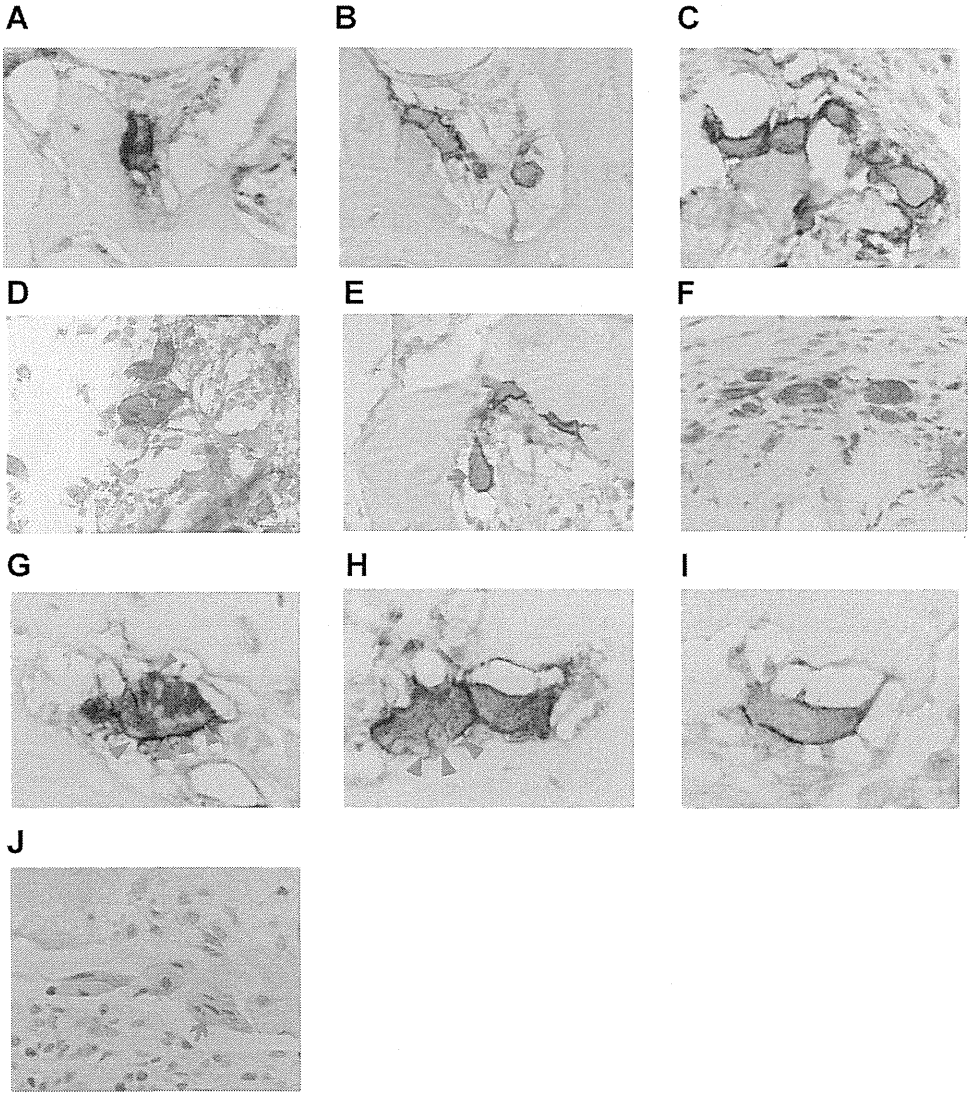

Fig. 1. Human osteoclasts (OCs) in both normal and pathological bone marrow are stained with CD26. (*A*) TRAP-stained human OC with membranous and cytoplasminc expression pattern; (*B*) CD26-stained human OCs with membranous and cytoplasmic expression pattern. Intensely CD26-stained human activated OCs were observed in the bone marrow; (*A*) and (*B*) Normal vertebra tissues without bone alterations. (*C*) Bone fractures with membranous and cytoplasmic CD26 expression pattern; (*D*) Osteosarcoma with membranous and cytoplasmic CD26 expression pattern; (*E*) Adenocarcinoma with membranous and cytoplasmic CD26 expression pattern; (*F*) Multiple myeloma (MM) with membranous and cytoplasmic CD26 expression pattern; (*G*) TRAP (blue stained)/CD26 (brown stained)-double stained OCs with membranous and cytoplasmic expression pattern; (*H*) TRAP (blue stained)/Vitronectin receptor (brown stained)-double stained OCs with membranous and cytoplasmic expression pattern; (*I*) TRAP (blue stained)/Calcitonin receptor (brown stained)-double stained OCs with membranous and cytoplasmic expression pattern; (*J*) IgG control. (*G–J*) OCs in bone granulation tissues of bone fractures. (*E, J*) Arrows (red) show multinuclear OCs. (*G, H*) Arrowheads (red) show nucleus in multinuclear OCs (original magnification: *A–J* ×400).

and 6; protocol 1), from day 5 (on day 5, 7, 9 and 11; protocol 2), or from day 8 (on day 8, 10, 12 and 14; protocol 3) (Fig. 4*B*, 6*A*, 8*A*, S2).

Flow cytometric analysis

Cells were harvested using collagenase (Stem cell technologies, Vancouver, BC, Canada) and stained with various antibodies. Acquisition was performed using an EPICS XL/XL-MCL version 3.0 (Beckman Coulter, Brea, CA, USA) and data were analyzed using Flowjo software (TreeStar, Ashland, OR, USA). The following antibodies were used as primary antibodies: monoclonal anti-human CD26 (R&D Systems), anti-human CD26-Fluorescein (R&D Systems), anti-human RANK (R&D Systems) anti-human RANK-Phycoerythrin (PE) (Biolegend, San Diego, CA, USA), anti-human M-CSFR (R&D systems), anti-human M-CSFR-Biotin (eBioscience, San Diego, CA, USA), anti-human CD64-PE (BD Biosciences, San Jose, CA, USA), anti-human TRAP-Biotynylated (R&D Systems), anti-human CD206-PE (BD Biosciences). Other antibodies against monocyte-macrophage lineage related markers

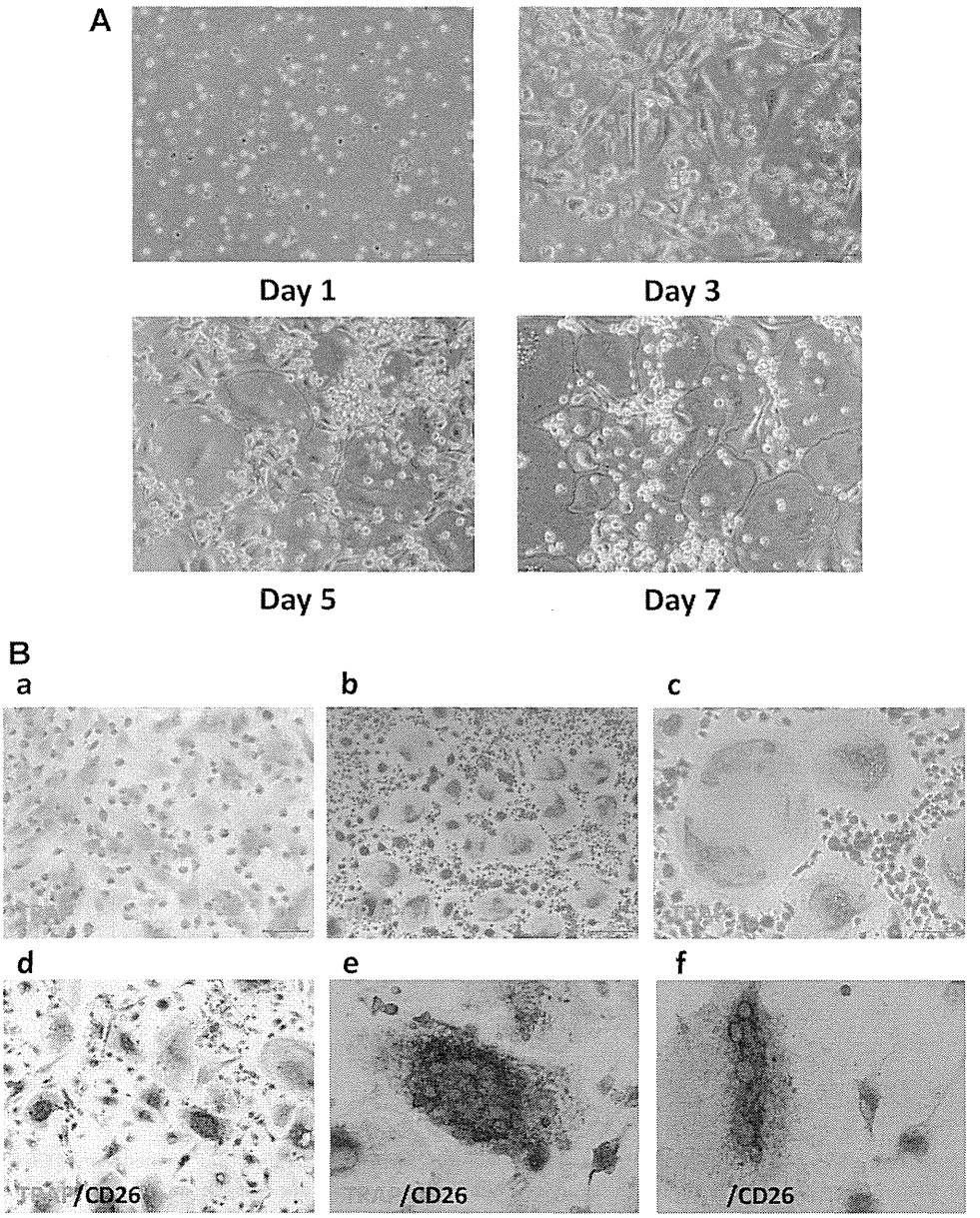

Fig. 2. Osteoclasts (OCs) derived from human bone marrow (BM) are stained with TRAP/CD26. (*A*) Human OC culture was performed. Photomicrographs of cultured cells on day 1, 3, 5 and 7 of human OC development are shown (original magnification: x100). (*B*) Photomicrograph of TRAP (red stained)-stained OCs derived from human BM-MNCs after 7 days of OC culture with human M-CSF (25 ng/ml) alone (a) or with human M-CSF (25 ng/ml) plus sRANKL (50 ng/ml) (*b–f*) are shown. (a) TRAP-negative cells are revealed. (b and c) TRAP (red stained)-stained human mature multinuclear OCs with cytoplasmic expression pattern and (d–f) TRAP (red stained)/CD26 (gray stained) double-positive human mature large OCs with cytoplasmic expression pattern of TRAP (red stained) and CD26 (gray stained) are demonstrated (original magnification: (a,b,d) ×100, (c,e,f) ×400).

were additionally used (see supplementary Materials and Methods). Polyclonal goat anti-mouse immunoglobulins/FITC goat F(ab')$_2$ (DAKO, Carpinteria, CA, USA), FITC goat anti-rat IgG (R&D Systems) and streptavidin PerCP (BD Biosciences) were used as secondary antibodies. To detect cellular proliferation in monocyte-macrophage lineage cells, OC culture was performed with human BM-MNCs, labeled with carboxy fluorescein diacetate succinimidyl ester (CFSE; Molecular Probes, Carlsbad, CA, USA). On day 0, 1, and 3, cells were harvested and analyzed using an EPICS XL/XL-MCL version 3.0 (Beckman Coulter).

PCR amplification and reverse-transcribed mRNA (RT-PCR)

Cells were harvested using collagenase (Stem cell technologies). Total cellular RNA of OC precursor cells and OCs was extracted

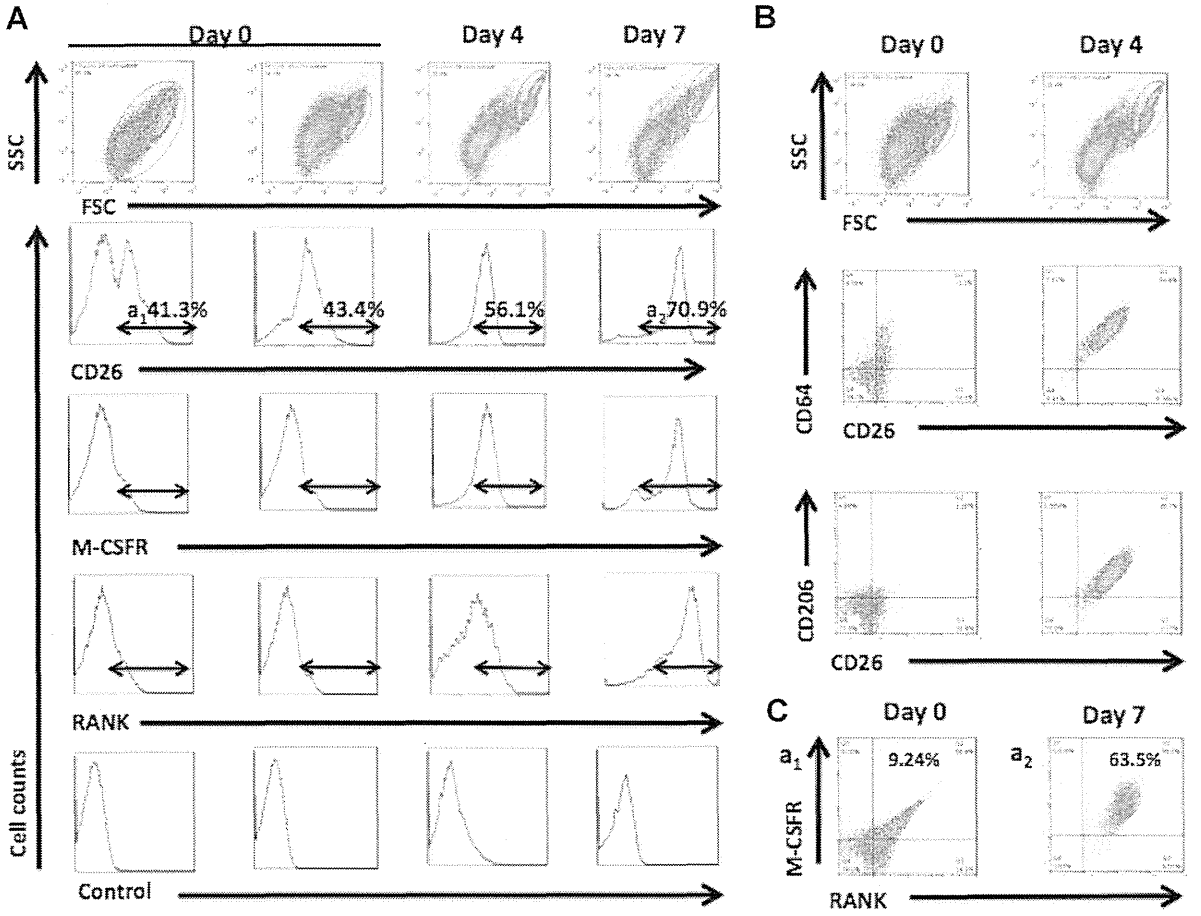

D

	CD26+	M-CSFR+	RANK+	CD26+/M-CSFR+/RANK+
Day 0	43.4+/-2.7	16.3+/-2.1	11.6+/-1.3	9.24+/-1.1
Day 4	56.1+/-1.7	53.1+/-2.0	40.7+/-2.3	33.8+/-1.6
Day 7	70.9+/-2.0	83.5+/-1.5	74.9+/-2.2	63.5+/-2.1

Fig. 3. CD26 expression is increased in association with monocyte-macrophage marker expressions during human osteoclast (OC) development. Levels of human CD26, M-CSFR, RANK, CD26/CD64, CD26/CD206, and CD26/M-CSFR/RANK on the cell surface during human OC development were analyzed by flow cytometry ($n = 3$). The cells were first live-gated on forward and side scatter plots. (*A*) On day 0, human BM-MNCs were stained positive for CD26 (a_1: 41.3%), M-CSFR and RANK. On day 4, increased levels of CD26, M-CSFR and RANK expression in monocytes-macrophage lineage cells were detected. On day 7, mature multinuclear OCs differentiated and proliferated. CD26 (a_2: 70.9%), M-CSFR and RANK expression reached their maximum levels. (*B*) On day 0, in monocyte-macrphage lineage cells, CD26/CD64 double stained cells were detected, but the ratio of CD26/CD206 double-stained cells was low. On day 4, the ratios of both CD26/CD64 double-stained cells and CD26/CD206 double-stained cells, indicative of OC precursor cells were gradually increased. (*C*) Three-color flow cytometry results were obtained on day 0 and day 7 of human OC culture. CD26-stained cells were gated, and further analyzed for M-CSFR and RANK. Triple staining showed that the cells express CD26, M-CSFR and RANK (day 0: 9.24%, day 7: 63.5%). (*D*) The table below the histogram shows the average of CD26+, M-CSFR+, and RANK+ population (%) ± standard deviation from 3 independent experiments.

using an RNeasy Micro Kit (Qiagen, Valencia, CA, USA), according to the manufacturer's protocol. cDNA was synthesized from total RNA with oligo $(dT)_{12\text{-}18}$ primers and subjected to PCR amplification using a Superscript III First-Strand Synthesis System Kit (Life Technologies). The PCR reactions were performed using a Veriti Thermal Cycler (Applied Biosystems, Foster, CA, USA) as follows: 94°C for 4 minutes, then denaturing at 98°C for 10 seconds, annealing at 55°C for 30 seconds, and extending at 72°C for 1 minutes for 35 cycles. The PCR products were separated by electrophoresis on 2% agarose gels and were visualized by ethidium bromide staining with UV light illumination.

qRT-PCR was performed on Thermal Cycler Dice (Takara) with SYBR Premix Ex Taq II (Takara, Tokyo, Japan) according to standard PCR conditions. The relative expression of selected genes was normalized to that of β-actin for each sample. The

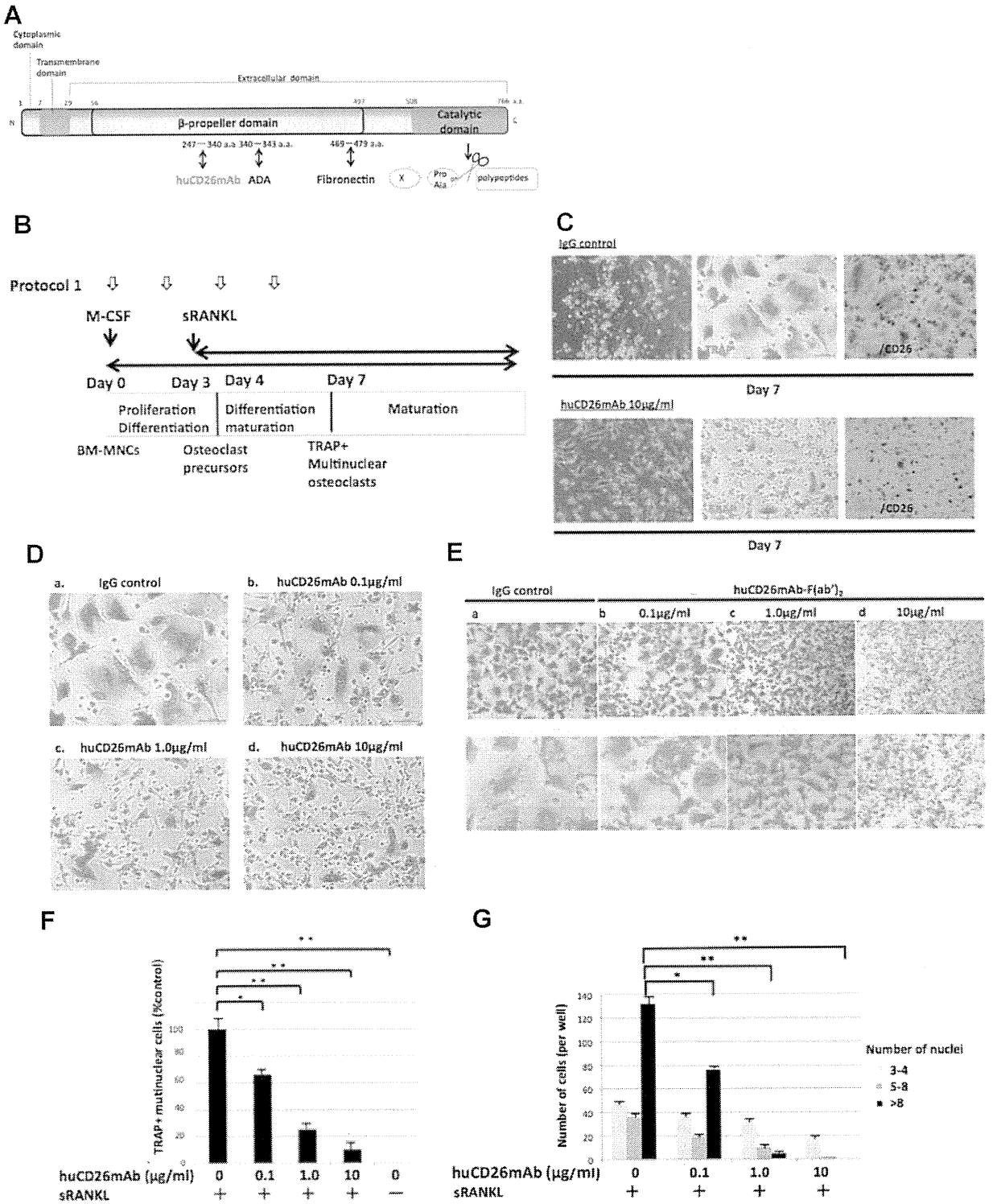

sequences of the primers used in PCR analysis are shown in the supplementary materials and methods.

Immunoblotting

Cells were harvested using collagenase (Stem Cell Technologies) and lysed with ice-cold RIPA buffer, containing 50 mM Tris-HCl (pH 7.5), 150 mM NaCl, 1.25% NP-40, 0.1% SDS, and protease inhibitor (Roche, Mannheim, Germany). Whole cell extracts were prepared by centrifugation at 15,000 rpm for 10 minutes at 4°C to pellet cellular debris. Whole cell extracts (30 μg) were subjected to a 7.5% SDS-poly-acrylamide gel electrophoresis (Life Technologies) and were transferred to a PVDF membrane (GE Healthcare, Buckinghamshire, UK). Nuclear extracts were prepared using NE-PER Nuclear and Cytoplasmic Extraction Reagents (Thermo Scientific, Rockford, IL, USA). The primary antibodies used were as follows: human CD26 with goat polyclonal antibody (R&D Systems), M-CSFR (Cell Signaling Technology), NF-κB (Cell Signaling Technology), NFATc1 (Santa Cruz Technology, Santa Cruz, CA, USA), DC-STAMP (Santa Cruz Biotechnology), Cathepsin K (Santa Cruz Biotechnology), αv-Integrin (Cell Signaling Technology), Src (Cell Signaling Biotechnology), MMP-9 (Cell Signaling Technology), β-actin (Sigma Aldrich), p38 MAPK (Cell Signaling Technology), phopho-p38 MAPK (Cell Signaling Technology), p44/42MAPK (Cell Signaling Technology), phospho-p44/42 MAPK (Cell Signaling Technology), SAPK/JNK (Cell Signaling Technology), phospho-SAPK/JNK (Cell Signaling Technology), MKK3/MKK6 (Cell Signaling Technology), phospho-MKK3/MKK6 (Cell Signaling Technology), mi/Mitf (Santa Cruz Biotechnology) and phospho-mif/Mitf (Biotec). Horseradish peroxidase-conjugated goat anti-rabbit IgG-HRP (Cell Signaling Technology) and horseradish peroxidase-conjugated goat anti-mouse IgG-HRP (Cell Signaling Technology) were used as secondary antibodies. The membranes were incubated with ECL immunoblotting detection reagents (GE Healthcare) followed by exposure to hyperfilm (GE Healthcare).

Tartrate-resistant acid phosphatase (TRAP-5b) and type1 collagen (CTX) activity assay

Human OC culture was performed without changing culture media or cytokine supplementation. On day 7, supernatants in the cultured medium were recovered and collected as described above by centrifuging for 15 minutes at 1000 g and used as samples for TRAP-5b and CTX quantitative assay. TRAP-5b and CTX concentrations were quantified using a human TRACP-5b ELISA Kit (Cosmo Bio, Carlsbad, CA, USA) and human CTX ELISA Kit (ACEL, Kanagawa, Japan), according to the manufacturer's instructions.

Calcium phosphate substrate resorption activity assay

Human OC culture was performed in fluoresceinated calcium phosphatase-coated 24-well plates. On day 14, human OC function was assayed by measuring calcium phosphate substrate resorption activity. Calcium phosphate substrate resorption activity was evaluated by measuring the fluorescence intensity of the conditioned medium using a Bone Resorption Assay Kit (PG Research, Tokyo, Japan), according to the manufacturer's instructions.

Statistical Analysis

All statistical analyses were performed using a two-tailed Student's *t*-test. *P* values less than 0.05 were considered statistically significant. Data are presented as mean values with 95% confidence intervals. Results are representative of three individual experiments.

Results

CD26 stained osteoclasts (OCs) are demonstrated in human bone marrow

To evaluate human OC development *in vivo*, immunohistochemical staining of CD26 and TRAP in human bone marrow tissues was performed. The expressions of TRAP and CD26 in OCs were observed in the human bone marrow of normal vertebra without bone alterations (Fig. 1*A*, *B*). We further examined CD26 expression in pathological human bone marrow tissues. Intensely CD26-stained activated OCs were observed in human bone marrow with bone fractures (Fig. 1*C*), osteosarcoma (Fig. 1*D*), adenocarcinoma (Fig. 1*E*), MM (Fig. 1*F*), further supporting a role for CD26 in human OC development. Furthermore, human OCs stained with TRAP/CD26, TRAP/

Fig. 4. Humanized anti-CD26 monoclonal antibody (huCD26mAb) blocks human osteoclast (OC) development. (*A*) CD26 is composed of a short cytoplasmic domain, a transmembrane region and an extracellular domain with dipeptidyl peptidase IV activity, which selectively removes the NH_2-terminal dipeptide from polypeptides containing either a proline or alanine at the penultimate residue. The epitope recognized by huCD26mAb is located at the cell membrane proximal glycosylated region, comprising the 247th–340th amino acid regions of human CD26. (*B*) Human OC culture was performed in the absence or presence of huCD26mAb (0, 0.1, 1.0, 10 μg/ml). huCD26mAb was added every 48 hours, for a total of 4 doses from day 0 (on day 0, 2, 4 and 6; protocol 1)(see Materials and Methods). (*C*) Human OC development in the absence or presence of huCD26mAb, using protocol 1 is shown. In human OC culture in the presence of huCD26mAb (10 μg/ml), on day 7, multinuclear mature OC differentiation was blocked. TRAP (red stained) and TRAP (red stained)/CD26 (gray stained) double-stained images of day 7 cultures in the absence or presence of huCD26mAb are shown (original magnification: ×100). (*D*) Photomicrographs of TRAP (red stained)-stained mature OCs in human OC culture on day 7, in the absence or presence of huCD26mAb, using protocol 1 (D: a: 0, b: 0.1, c: 1.0, d: 10 μg/ml) are shown (*D*: a-d original magnification ×100). huCD26mAb dose-dependently inhibited both TRAP (red stained)-stained mature OC differentiation (a-d: TRAP enzyme-histochemistry). (*E*) The effect of huCD26mAb-F(ab′)$_2$ on human OC development was analyzed. Photomicrographs of TRAP (red stained)-stained mature human OCs on day 7 of OC culture in the absence or presence of huCD26mAb-F(ab′)$_2$ (a: 0, b: 0.1, c: 1.0, d: 10 μg/ml), using protocol 1, are shown (both original magnifications, a–d: ×40, ×100). huCD26mAb dose-dependently blocked TRAP-stained mature OC differentiation (a–d: TRAP enzyme-histochemistry). (*F, G*) The number of TRAP+ multi-nuclear OCs (>3 nuclei) were quantified. huCD26mAb (0.1, 1.0, 10 μg/ml)-treated versus non-treated (0 μg/ml) human OC culture using protocol 1 was shown to exhibit decreased human OC development in a dose-dependent manner, as shown by significantly lower numbers of small (3 or 4 nuclei/OC), medium (5–7 nuclei/OC), and large (>8 nuclei/OC) OCs. Data represent the means ± SD. $n = 3$. $^*p < 0.05$, $^{**}p < 0.01$.

Vitronectin receptor or TRAP/Calcitonin receptor were also demonstrated in bone granulation tissues of bone fractures (Fig. 1*G, H, I*). These findings demonstrate that CD26 is expressed in human OCs and is intensely expressed in OCs with osteolytic bone metastasis.

CD26 expression during human osteoclast (OC) development

The culture of human BM-MNCs with M-CSF plus sRANKL (OC culture) results in the differentiation of OC precursor cells from

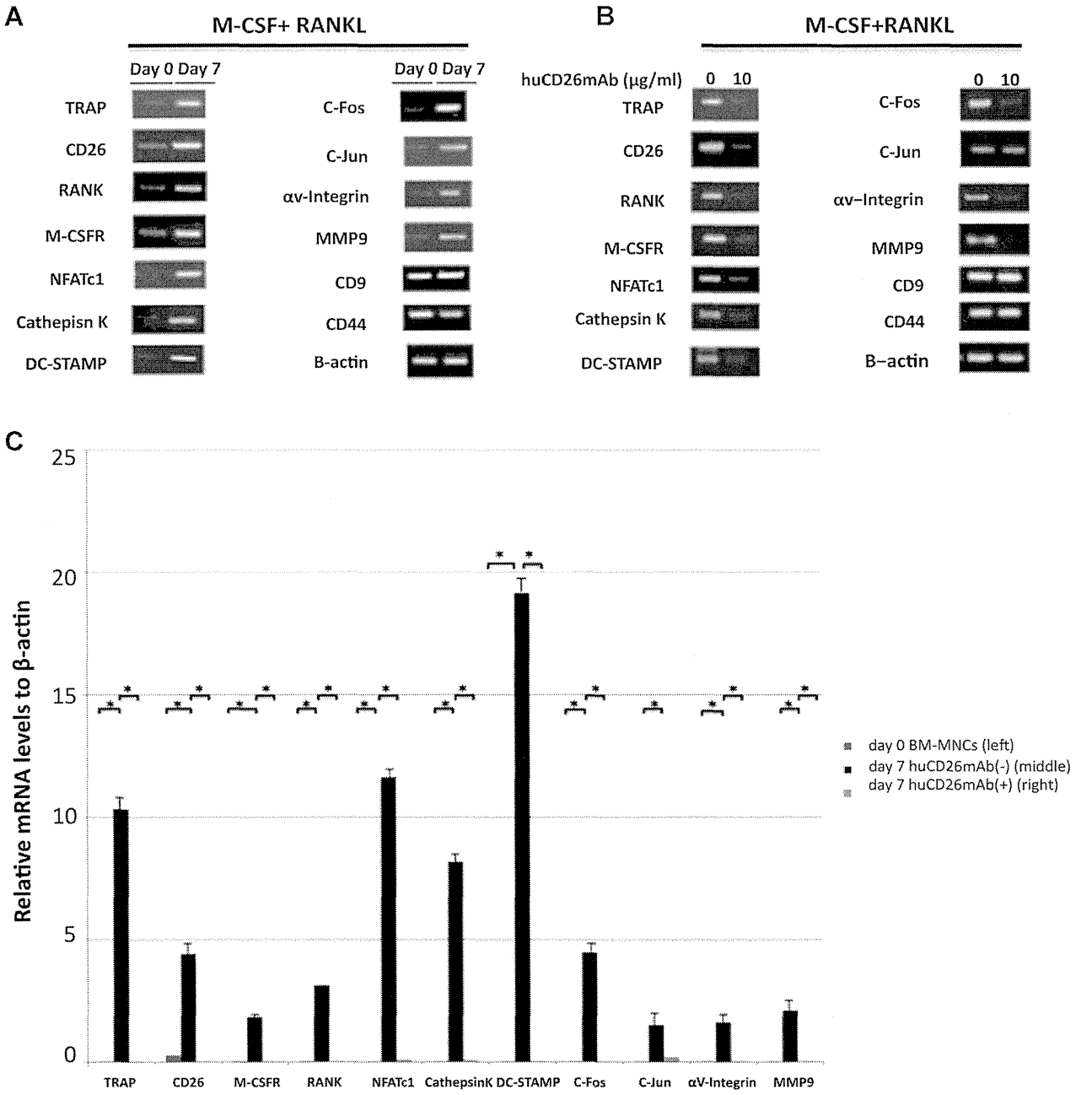

Fig. 5. Gene expression analysis. (*A*) Gene expression in human OC development. Human OC culture was performed to collect total RNA from BM-MNCs on day 0 and OCs on day 7, as described in Materials and Methods and RT-PCR was performed to detect the expression of the indicated genes correlating with human OC development. Gene expression of TRAP, CD26 and other genes related to OC development were increased in human OCs. (*B*) Gene expression in human OC development in the absence or presence of huCD26mAb. Human OC culture was performed in the presence of huCD26mAb (10 μg/ml) using protocol 1 for 7 days to collect total RNAs of human OCs and cultured cells on day 7 and to RT-PCR was performed. The expressions of the indicated osteoclastic genes, such as TRAP, CD26, M-CSFR, RANK, NFATc1, Cathepsin K, DC-STAMP, c-Fos, αv-Integrin and MMP9 in cultured cells were inhibited in OC culture with huCD26mAb. (*C*) Normalized (to β-actin) levels of osteoclastic and other genes from day 0 (BM-MNCs) and day 7 of human OC culture with M-CSF plus sRANKL were measured by RT-qPCR in the absence or presence of huCD26mAb (10μg/ml) using protocol 1; $n = 3$. Data represent the mean ± SD. $n = 3$. $^*p < 0.05$.

monocyte-macrophage lineage cells and their fusion into bone-resorbing multinuclear OCs. To identify the role of CD26 in human OC development, we first evaluated the expression of CD26 in human BM-MNCs, monocyte-macrophage lineage cells, OC precursor cells and OCs. The results showed that mature human multinuclear OCs were stained positive for both TRAP and CD26 (Fig. 2*A*, *B*). Flow cytometric analysis also revealed that the addition of M-CSF plus sRANKL induced human OC differentiation, in association with the expression of CD26 in monocyte-macrophage lineage cells and OC precursor cells. The ratios of CD26, M-CSFR, RANK, CD26/CD64, and CD26/CD206 double-stained cells, indicating human OC precursor cells, were increased on day 4 (Fig. 3*A*, *B*, *D*). Expressions of other monocyte-macrophage lineage related markers in OC precursor cells became also increased (Fig. S1). Furthermore, the ratios of CD26-stained cells and CD26/M-CSFR/RANK triple-stained cells, indicating OC precursor cells and mature OCs, were increased to 89.5% of all CD26+ cells (63.5%) on day 7 (Fig. 3*C*, *D*). These data indicate that M-CSF and RANKL induced human OC differentiation in association with the up-regulation of CD26 expression in monocyte-macrophage lineage of hematopoietic cells.

Humanized anti-CD26 monoclonal antibody (huCD26mAb) impairs human osteoclast (OC) development

To determine the effects of huCD26mAb on human OC development, human OC culture was performed, in the absence or presence of huCD26mAb (0.1, 1.0, 10 μg/ml) (protocol 1, Fig. 4*A*, *B*). On day 7 of human OC culture, multinuclear OC differentiation and maturation were blocked. The number of TRAP-stained multinuclear OCs was significantly reduced in the presence of huCD26mAb in a dose-dependent manner (Fig. 4*C*, *D*). The number of TRAP-positive mature multinuclear OCs was decreased to 65% ± 10% ($p < 0.05$), 22% ± 7% ($p < 0.05$) and 7% ± 3% ($p < 0.05$) upon treatment with huCD26mAb of 0.1 μg/ml, 1.0 μg/ml, and 10 μg/ml, respectively (Fig. 4*F*). In the presence of huCD26mAb, significantly reduced numbers of small (3 or 4 nuclei/cell), medium (5–7 nuclei/cell), and large (>8 nuclei/cell) OCs were generated in human OC culture (Fig. 4*G*). Our data show that huCD26mAb dose-dependently impairs human OC formation. We also generated and purified huCD26mAb-F(ab')$_2$, lacking the Fc portion by pepsin digestion. When human OC was performed in the absence or presence of various concentrations of huCD26mAb-F(ab')$_2$ (0, 0.1, 1.0, 10 μg/ml), huCD26mAb-F(ab')$_2$ also dramatically blocked human OC differentiation and subsequent maturation in a dose-dependent manner (Fig. 4*E*). These data indicate that the inhibitory effects of huCD26mAb on human OC differentiation are independent of the Fc function of huCD26mAb.

We next analyzed the gene expression profiles of various candidate genes that correlate with human OC development. OC precursor cells were cultured with M-CSF plus RANKL for 2 to 4 days, resulting in the generation of TRAP-positive multinuclear mature OCs. The expressions of CD26, c-Fos, c-Jun, and NFATc1 were up-regulated after RANKL stimulation (Fig. 5*A*). In addition, the expression of various osteoclastic genes, including Cathepsin K, DC-STAMP, αv-Integrin and MMP9, was up-regulated in mature OCs on day 7 of OC culture (Fig. 5*A*, *C*). We also determined the impact of huCD26mAb (10 μg/ml) on human OC development by measuring the expression of osteoclastic genes. The expressions of CD26, c-Fos, and NFATc1 were down-regulated after RANKL stimulation, but the expression of c-Jun remained unchanged. In addition, the expressions of Cathepsin K, DC-STAMP, Src, αv-Integrin, and TRAP were also down-regulated (Fig. 5*B*, *C*).

huCD26mAb blocks early human osteoclast (OC) precursor differentiation into OCs

To determine which phase of OC development is affected by huCD26mAb, human OC culture was performed with 10 μg/ml of huCD26mAb for four consecutive 48-hour intervals on day 0, 2, 4, and 6 of OC culture (protocol 1), day 5, 7, 9, and 11 (protocol 2), or day 8, 10, 12, and 14 (protocol 3) (see Materials and Methods) (Fig. 6*A*, S2). Impaired mature multinuclear OC formation could have resulted from the impairment of either (1) the phase of monocyte-macrophage lineage cell differentiation and proliferation, (2) the early phase of OC differentiation, or (3) the late phase of OC differentiation and maturation. On day 7, the ratio of CD26 stained cells was reduced to 14.8% of total cells and the ratio of CD26/M-CSFR/RANK triple-stained cells indicative of human OC precursor cells and mature OCs was significantly decreased in huCD26mAb-treated OC culture (Fig. 6*B*, *C*, *D*). To rule out the possibility that huCD26mAb affects the differentiation and proliferation of monocytes and macrophages derived from human BM-MNCs, we performed OC culture using CFSE-labeled human BM-MNCs in the absence or presence of huCD26mAb (10 μg/ml), and CFSE intensity was analyzed for cell division as a reflection of proliferation activity. The formation of monocyte-macrophage lineage cells in human OC culture was similar regardless of the absence or presence of huCD26mAb (Fig. 6*E*). Taken together, these findings indicate that huCD26-mAb blocks human OC differentiation or maturation, but not monocyte-macrophage differentiation or proliferation. Moreover, cell fusion is a critical phase in OC maturation, and multinuclear OC development is required for OC function. However, treatment with huCD26mAb during the phase of OC maturation and proliferation in OC culture, as was shown in protocol 2 or protocol 3, did not significantly alter OC formation (Fig. S2). In fact, the ratio of CD26/M-CSFR/RANK triple-stained OCs, indicating OC precursor cells and mature OCs, was not shown by flow cytometry to be decreased on day 7 (Fig. 6*C*). An increase in the number of TRAP/CD26-stained multinucleated mature OCs was also demonstrated in OC culture in the presence of huCD26mAb, as was shown in protocol 2 and protocol 3 (Fig. 6*F*, S2). huCD26mAb also dose-dependently decreased the level of TRAP expression on the cell surface of human OCs cultured in the presence of huCD26mAb under protocol 1, but not under protocol 2 (Fig. 6*G*). These results indicate that huCD26mAb affects the early phase of OC precursor cell differentiation into OCs but not OC maturation.

huCD26mAb down-regulates the p38 MAPK-mediated signaling pathway, involved in early human osteoclast (OC) precursor differentiation

To determine whether huCD26mAb is associated with the failure of human OC differentiation, we first examined the expression of proteins correlated with human OC development using immunoblotting analysis. The expression of CD26, NFATc1, and OC fusion proteins, including DC-STAMP, Cathepsin K, αv-Integrin, Src, and MMP9, was reduced in human OCs in the presence of huCD26mAb (Fig. 7*A*).

We further examined the effects of huCD26mAb on the phosphorylation of MAPKs of the RANK signaling pathway in

human OC precursor cells and mature OCs. Time-course changes in the phosphorylation of MKK3/6, p38 MAPK, ERK, SAPK/JNK, and IKK_B in response to RANKL are shown in Fig. 7*B*. In response to RANKL stimulation, MKK3/6 and p38 MAPK were phosphorylated within 15 minutes, in human OC precursor cells and reached a maximum level within 30 minutes, which was maintained for up to 60 minutes (Fig. 7*B*). Moreover, nuclear extracts were prepared and mi/Mitf phosphorylation was simultaneously examined using

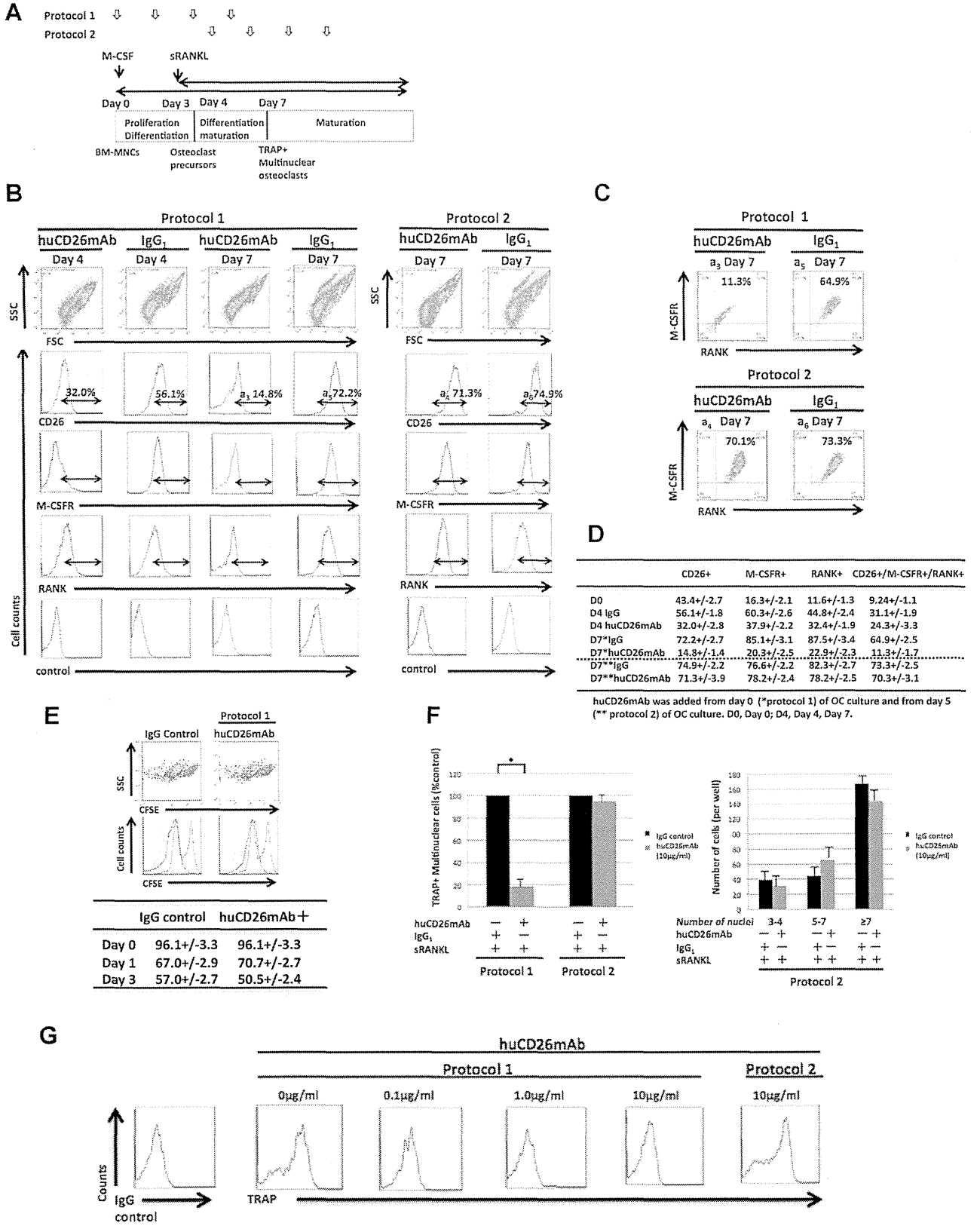

anti-phospho-mi/Mitf antibody. mi/Mitf was subsequently rapidly activated in human OC precursor cells and persisted for 24 hours (Fig. 7C). When huCD26mAb is bound to CD26 on human OC precursor cells, MKK3/6 and p38 MAPK were specifically and rapidly inactivated, starting within 15 minutes of RANKL stimulation, as shown by the persistent decrease in the phosphorylation of p38 MAPK, together with MKK3/6. Subsequent mi/Mitf phosphorylation was also persistently inhibited, which is consistent with the lack of p38 MAPK phosphorylation in OCs on day 7 of human OC culture (Fig. 7C, S3). huCD26mAb-F(ab')$_2$ also dramatically blocked human OC differentiation and subsequent maturation in a dose-dependent manner by inhibiting the p38 MAPK-mi/Mitf phosphorylation pathway in human OC precursor cells (Fig. 4E, S4). Phosphorylation of other MAPKs, including ERK, SAPK/JNK, or IKK$_B$, was rapidly induced in response to RANKL in human OC precursor cells, regardless of the absence or presence of huCD26mAb. These results indicate that the potential mechanism of action involved in the impairment of early osteoclast differentiation by huCD26mAb results from the blockade of the p38 MAPK-mi/Mitf phosphorylation pathway in human OC precursor cells and fusion proteins in human OCs are subsequently down-regulated, thereby inhibiting human OC fusion and functions (Fig. 7A, B, C).

p38 MAPK inhibitor blocks human osteoclast (OC) differentiation

To examine the role of p38 MAPK in RANK-RANKL mediated human OC differentiation, we examined the inhibitory effects of a specific inhibitor of p38 MAPK, SB203580, on human OC development. Human OC culture, performed in the absence or presence of varying concentrations of p38MAPK inhibitor, SB203580 (10, 20, 100 μM) for the indicated times, resulted in a dose-dependent inhibition of cell adhesion (Fig. 7D, S5). Furthermore, in human OC precursor cells, treatment with SB203580, using protocol 1 strongly inhibited human OC formation through the suppression of p38 MAPK phosphorylation and subsequent mi/Mitf activation in response to RANKL (Fig. 7B). In contrast, the addition of SB203580 using protocol 2 failed to inhibit osteoclastgenesis, consistent with the lack of p38 MAPK phosphorylation in OCs on day 7 of human OC culture (Fig. 7D, S3). The expression of CD26 in human OCs was also reduced in the presence of SB203580, in a dose-dependent manner (Fig. S3). These results demonstrate that p38 MAPK-mediated signals are essential for inducing early human OC precursor differentiation into OCs, but not for OC maturation, indicating that human OC maturation and function is induced through a mechanism independent of p38 MAPK mediated signaling.

DPPIV inhibitor has no significant effects on human osteoclast (OC) development

DPPIV enzymatic activity is required for CD26-mediated T cell co-stimulatuin. We examined the efficacy of the DPPIV inhibitor, Vidagliptin, on human OC development. Vidagliptin had no significant inhibitory effect on human OC differentiation or maturation (Fig. 7E, F) and did not affect human OC functions (data not shown). These results indicated that the mechanism of action by huCD26mAb on human OC development does not correlate with the reduction in DPPIV enzymatic activity in CD26.

huCD26mAb does not directly affect functions of mature OC

The development of multinuclear OCs is necessary for efficient OC functions. To determine whether huCD26mAb also affects the bone resorption activity of human multinuclear OCs, we examined the formation of resorption pits on human mature multinuclear OCs. First, calcium phosphate substrate resorption activity assay was performed in the absence or presence of various concentrations of huCD26mAb (0, 0.1, 1.0, 10 μg/ml), using protocol 1, protocol 2, and protocol 3 (see Materials and Methods) (Fig. 8A). It was observed that in human OC culture without huCD26mAb, OCs spread on the fluoresceinated calcium phosphate-coated plates with large resorption pit area, showing bone resorptive activity, whereas in OCs cultured with huCD26mAb or huCD26mAb-F(ab')$_2$

Fig. 6. huCD26mAb inhibits early osteoclast (OC) precursor differentiation, but does not influence late phase OC maturation. (*A*) Human OC culture was performed in the absence or presence of huCD26mAb (0, 0.1, 1.0, 10 μg/ml). huCD26mAb was added every 48 hours, for a total of 4 doses from day 0 (on day 0, 2, 4 and 6; protocol 1), from day 5 (on day 5, 7, 9 and 11; protocol 2), (see Materials and Methods). (*B*) The effects of huCD26mAb or isotype control; IgG$_1$ on the cell surface levels of CD26, M-CSFR and RANK in human OC development were analyzed by flow cytometry. In human OC culture in the presence of huCD26mAb (10 μg/ml), using protocol 1, on day 4, the levels of monocyte-macrophage lineage cells which were stained positive for CD26, M-CSFR and RANK were increased. However on day 7, the levels of CD26, M-CSFR and RANK in OCs or cultured cells became reduced. In OC culture with huCD26mAb, using protocol 2, on day 7, those of CD26, M-CSFR and RANK in OCs were not remarkably reduced. (*C*) On day 7, CD26-stained cells were gated and further analyzed for M-CSFR and RANK. Triple-staining showed that these cells express CD26, M-CSFR and RANK. The levels of CD26/M-CSFR/RANK triple-stained OCs were also markedly decreased (a_3: 11.3%). In contrast, in human OC culture with huCD26mAb using protocol 2, expressions of CD26, M-CSFR and RANK reached maximum level. CD26-stained cells were gated and showed that the levels of CD26/M-CSFR/RANK triple-stained OCs were increased (a_4: 70.1%). (*D*) The table below the histogram shows the average of CD26 +, M-CSFR +, and RANK+ population (%) ± standard deviation from 3 independent experiments. (*E*) To analyze cell proliferation in monocyte-macrophage lineage cells, human OC culture derived from CFSE-labeled human BM-MNCs was performed in the absence or presence of huCD26mAb (10 μg/ml), using protocol 1. Cultured cells on day 0, 1 and 3 were harvested and subjected to flow cytometry. Representative dot plots and histograms of CD26 expression on day 0 (red line), 1 (blue line), and 3 (green line) are shown. (*F*) The number of TRAP+ multinuclear OCs (>3 nuclei) in human OC culture in the presence or absence of huCD26mAb (10 μg/ml), using protocol 1 or protocol 2, was quantified. Treatment with huCD26mAb, using protocol 1, resulted in a decreased number of TRAP+ multinuclear OCs. In contrast, treatment with huCD26mAb, using protocol 2 did not decrease the number of TRAP+ multinuclear OCs (left panel). The number of nucleus in TRAP+ multinuclear OCs was not remarkably different between OC culture regardless of the absence or presence of huCD26mAb, using protocol 2 (right panel). Data represent mean plus minus SD. $n = 3$.*$p < 0.01$. (*G*) The level of TRAP expression on the cell surface of OCs in human OC culture in the presence or absence of huCD26mAb, using protocol 1 or protocol 2, was analyzed by flow cytometry. The level of TRAP expression in OCs was decreased in the presence of huCD26mAb (0.1,1.0,10μg/ml) (protocol 1) in a dose-dependent manner, but was not decreased in OCs with huCD26mAb (protocol 2).

as was shown in protocol 1, failed to spread and exhibited impaired resorptive activity and significantly reduced resorption pit areas (Fig. 8*B*, *C*, *D*, S5). In contrast, treatment with huCD26mAb (10 μg/ml) in OC culture at the late phase of OC differentiation or maturation, using protocol 2 or protocol 3 had no significant effect on bone resorption pit area with bone resorption activity in mature OCs (Fig. 8*B*, *C*, *D*, S6).

Moreover, TRAP is intensely expressed in OCs, inflammatory macrophages, and dendritic cells. Two different forms of TRAP, known as TRAP-5a and 5b, circulate in human blood. TRAP 5b is derived from OCs. Type 1 collagen (CTX), a degradation product of bone collagen released into culture medium, provides a much faster and more convenient method for quantifying bone resorption and is an accurate indicator of total resorbed volume,

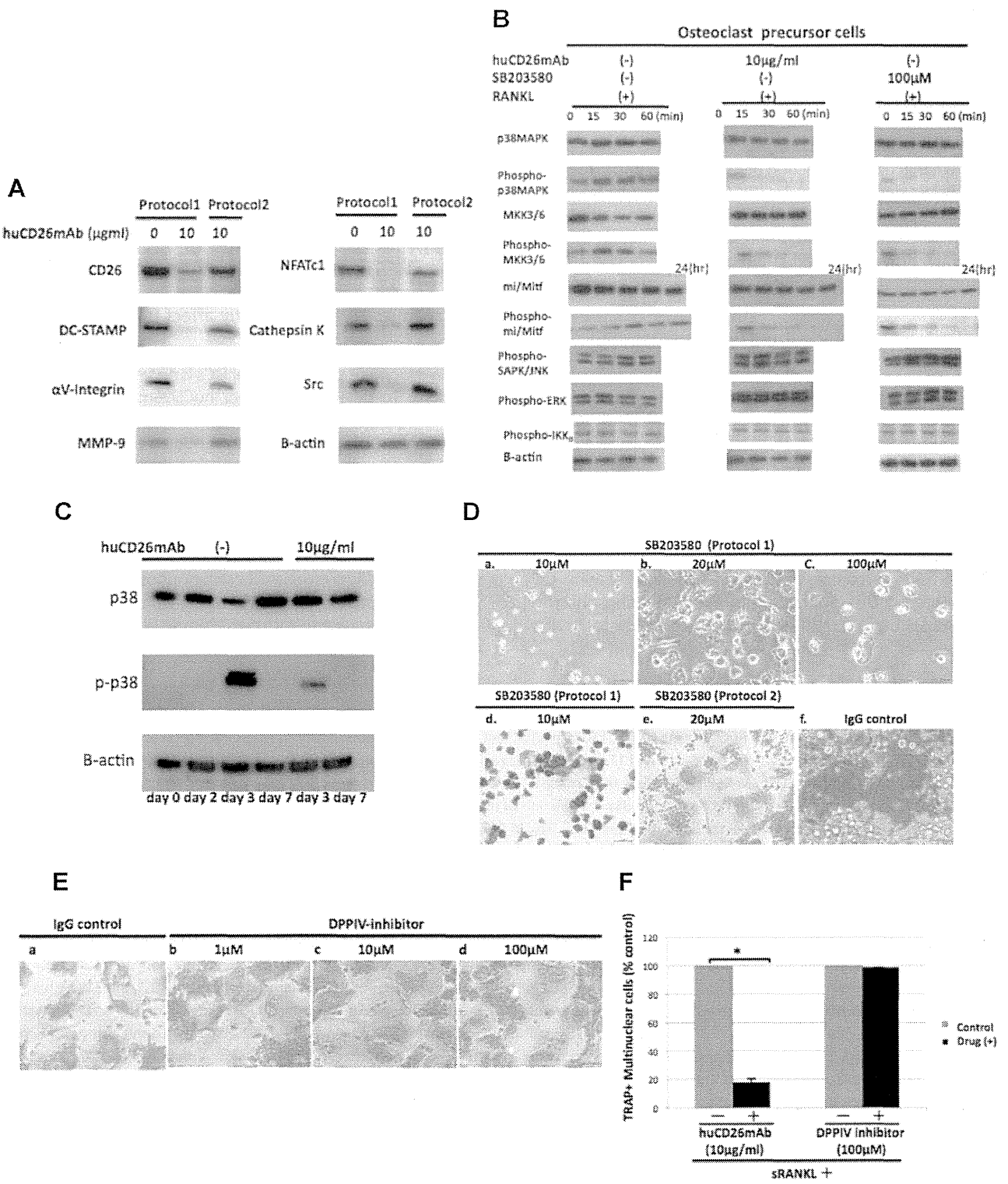

including both the area and depth of the formed resorption pits. TRAP-5b and CTX are adequate markers to quantify bone resorption activity in OCs and the levels of both TRAP-5b and CTX in human OCs cultured with either huCD26mAb or SB203580 were significantly reduced in a dose-dependent manner. In contrast, the addition of huCD26mAb during the phase of human OC maturation, using protocol 2, did not have its effect (Fig. 8*E*, *F*, *G*). These results indicate that huCD26mAb does not directly affect OC functions, but subsequently blocks human OC functions by inhibiting cell fusion, which is critical for human OC maturation, by down-regulating the CD26-p38 MAPK/mi/Mitf mediated signaling pathway in human OC precursor cells (Fig. 9).

Discussion

Bone remodeling is maintained by the delicate balance between OBs and OCs.[1–10,24–31] This study is the first report to show that CD26 plays a crucial role in human OC development. We identified the expression of CD26 in normal human OCs and CD26 was intensely detected in activated human OCs with osteolytic lesions following metastasis, including adenocarcinoma or MM and their related bone fractures. Furthermore, we clarified the roles and molecular mechanisms of CD26 in the function of OCs during human OC development, and the effects of CD26 blockade by huCD26mAb on human OC development and functions.

MAPK-mediated signals are also important for human OC differentiation. The MAPK family includes three subfamilies: p38 MAPK, ERK, and SAPK/JNK. The activation of these MAPK signaling pathways regulates various cellular processes, including cell proliferation, differentiation, survival and apoptosis.[14,15] p38 MAPK phosphorylation also occurs downstream of the RANK signaling pathway in OC precursor cells, during human OC development.[1,2,32–34] When p38 MAPK is activated, it stimulates and triggers the downstream activation of a key transcription factor, mi/Mitf. mi/Mitf up-regulates the expression of target genes encoding TRAP and plays an important role in OC function such as bone resorption activity.[35,36] It has been hypothesized that the phosphorylation of mi/Mitf on serine 307 in the p38 MAPK signaling pathway leads to a lower affinity for a co-repressor and subsequently increases the affinity of the interaction between mi/Mitf and PU.1 and increases the ability of transcription to stimulate OC differentiation.[34] The role of p38 MAPK differs in cells of origin and different states. In some cells, the target of p38 MAPK functions at the translational level, whereas in others, its target functions at the transcription level. In human OC development, p38 MAPK-mediated signals are essential for RANKL-induced differentiation of OCs but not dendritic cells from their common precursors.[37,38] p38 MAPK activation is also involved in pro-inflammatory cytokine production, including TNF and IL-1. In rheumatoid arthritis (RA), pro-inflammatory cytokines such as TNF-α, IL1-β, and IL-6 play a role not only in the inflammation but also in structural damage of the affected joints.[39,40] In this process, phospho-p38 MAPK is considered to control the production of inflammatory cytokines and to mediate the bone destructive properties of cytokines which leads to increased bone resorption of OCs.[39,40]

In several malignant lymphoma cells, the expression of CD26 is associated with constitutive phosphorylation of p38 MAPK. CD26 regulates integrinβ1 phosphorylation of T-cell lymphoma line, Karpass 299. In B-cell lymphoma line, Jiyoye, CD26 results in the increased levels of p38 MAPK phosphorylation and topoisomerase IIαexpression.[14,15] The mechanism as to how CD26 regulates p38 MAPK phosphorylation presently remains unclear.

Fig. 7. huCD26mAb inhibits the p38 MAPK-mediating osteoclastgenic signaling pathway in human OC precursor cells, but not in OC cells. (*A*) Immunoblotting results showing that levels of CD26 (110KDa), NFATc1(120KDa), and OC fusion-related proteins such as DC-STAMP (53KDa), Cathepsin K (37KDa), αv–Integrin(135KDa), Src (60KDa), MMP-9 (92KDa) are down-regulated after 7 days of human OC culture in the presence of huCD26mAb (10 μg/ml), using protocol 1. Down-regulation is not observed in cells subjected to protocol 2. Levels of the indicated proteins were evaluated by immunoblotting as described in Materials and Methods.Each lane contains the equal amount of proteins. (*B*) Time-course changes in the phosphorylation of MAPKs in human OC precursor cells and OCs after RANKL stimulation in the presence of huCD26mAb or the p38 MAPK inhibitor. In OC precursor cells, immediately after sRANKL (from day 3) was added, in response to RANKL, MKK3/6 (40KDa)-p38 MAPK(43KDa) phosphorylation was induced within 15 minutes and reached a maximum level within 30 minutes which was maintained for up to 60 minutes. mi/Mitf (52KDa) was subsequently rapidly activated and persisted for 24 hours. In contrast, in the presence of huCD26mAb (10 μg/ml), when huCD26mAb bound to CD26 on OC precursor cells, only the MKK3/6-p38 MAPK pathway was specifically rapidly inactivated. This was shown by the persistent decrease in the phosphorylation of p38 MAPK, together with MKK3/6, starting within 15 minutes of RANKL stimulation. Subsequent mi/Mitf phosphorylation was also persistently inhibited. These were consistent with a lack of MKK3/-p38 MAPK phosphorylation in mature OCs after RANKL stimulation, regardless of the absence or presence of huCD26mAb. Other MAPKs, including ERK, SAPK/JNK and NF-κB were rapidly activated in response to RANKL in OC precursor cells. (p-MKK3/6;40KDa, p-mi/Mitf;58KDa, p-SAPK/JNK;46,54KDa, p-ERK;42,44KDa, p-IKK_B;85KDa). (*C*) Time course expression of p38 MAPK and phospho-p38 MAPK (43KDa) during human OC culture as was shown above with or without huCD26mAb (10μg/ml). The expression of phospho-p38 MAPK was shown in OC precursor cells on day 3, but not in OCs on day 7 of OC culture. huCD26mAb inhibited the expression of phopho-p38MAPK in OC precursor cells on day 3 of OC culture. (*D*) The effects of the p38MAPK inhibitor on human OC development. Human OC culture was performed in the presence of the indicated concentrations of SB203580 (10, 20, 100 μM), dissolved in DMSO (0.4%) on collagen-coated 24-well plates. Following incubation, the plates were washed to remove non-adhesive cells. Photomicrographs of the remaining cells adhering to the collagen plates are shown. Mature OCs had not differentiated in the presence of SB203580 on day 7 of human OC culture. BM-MNCs cultured in the presence of SB203580, using protocol 2 (After human OC culture for 4 days, SB203580 (20 μM) was added to the cultured cells), had differentiated into mature OCs. (a–f: original magnification ×200, SB203580; a: 10 μM, b: 20 μM, c: 100 μM, d: 10μM, e: 20 μM, d, e: TRAP enzyme-histochemistry, f: IgG control) (*E*) The effects of DPPIV inhibitor on human OC development. Photomicrographs of TRAP (red stained)-stained mature OCs on day 7 of human OC culture are shown in the presence of the DPPIV inhibitor, Vildagliptin (a: IgG control, b: 1.0μM, c: 10μM, d: 100 μM), using protocol 1 (both original magnification, a-d: ×100). DPPIV inhibitor had no significant inhibitory effects on human OC development (a-d: TRAP enzyme-histochemistry). (*F*) The number of TRAP+ multinuclear OCs (>3 nuclei) in human OC culture in the presence of DPPIV inhibitor, Vildagliptin (100μM). Treatment with Vildagliptin did not decreased the number of TRAP+ multinuclear OCs in the presence of Vildagliptin as compared with huCD26mAb. Data represent mean plus minus SD. $n = 3$. $^*p < 0.01$.

CD26 is a serine protease capable cleaving selected biological factors, so it is possible that CD26 indirectly regulates p38 MAPK phosphorylation pathway via the activity of cleaved substrates. CD26 is also physically and functionally related to the molecules with key roles of signal transduction, such as the tyrosine phosphatase. CD26 may have several effects on p38 MAPK phosphorylation through their related molecules.[14,15]

huCD26mAb has high biological activity: it selectively binds human CD26 and suppresses the growth and invasion of malignant lymphoma cells and several solid tumor cells with no evidence for immune activation and no effect on DPPIV activity, and it induces long-term survival of a tumor-transplanted mouse model.[13–16] It has also been shown that huCD26mAb recognizes an epitope located at the cell membrane-proximal glycosylated region, formed by 247th–340th amino acid regions in human CD26, near the ADA binding domain[11,12] (Fig. 4*A*). Antibody-dependent cytotoxicity (ADCC) following binding of the antibody Fc region to the Fcγ-receptor (FcγR) on effector cells, and in particular NK cells, represents the major *in vivo* anti-tumor mechanism of action of anti-tumor therapeutic monoclonal antibodies, such as rituximab, trastuzumab, alemtuzumab, and mogamulizumab.[41–43] huCD26mAb has a human IgG_1

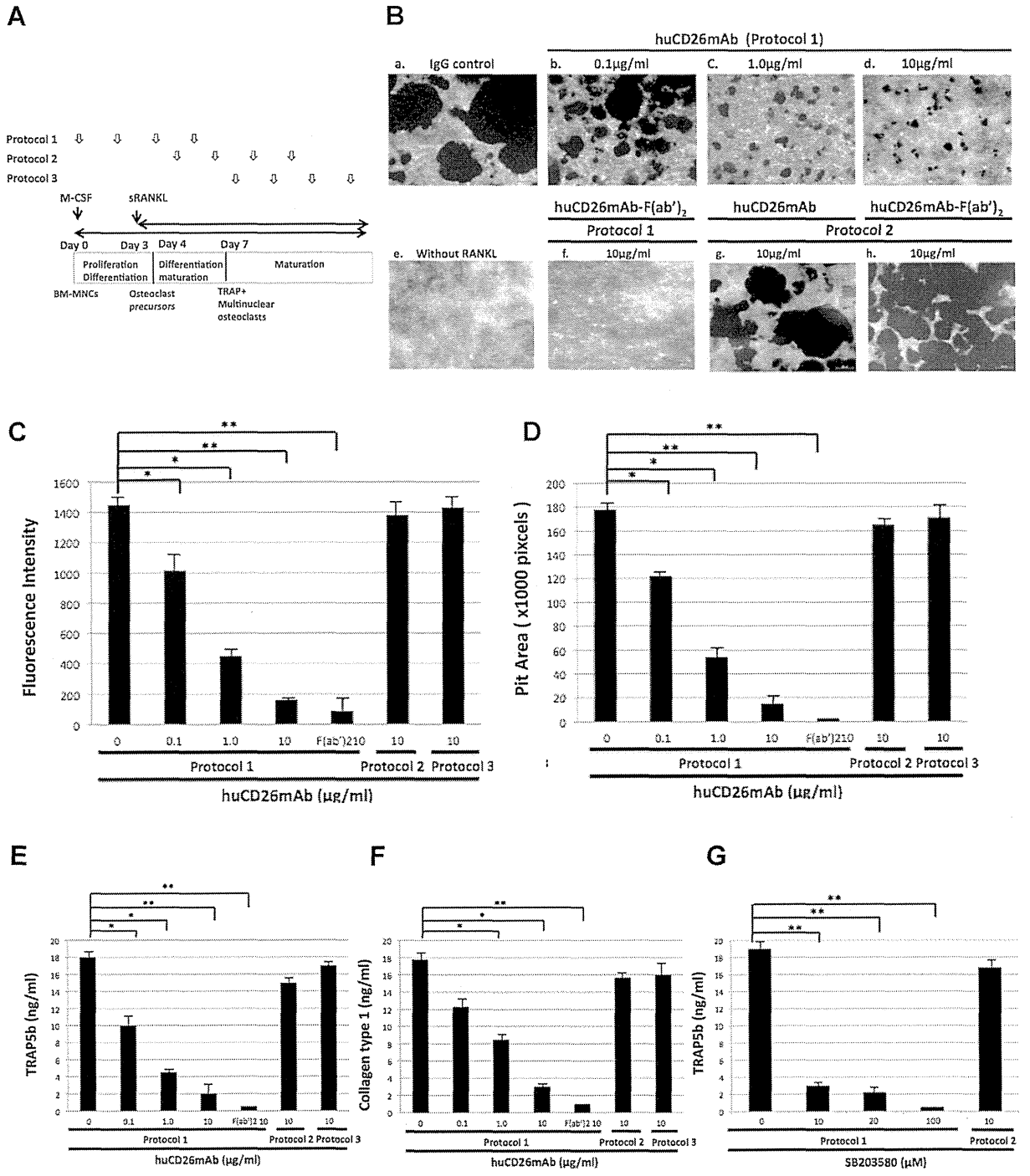

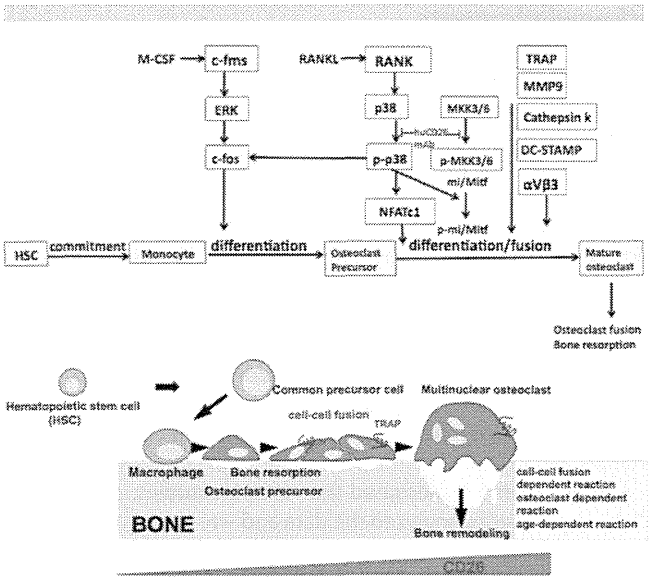

Fig. 9. Schematic proposed mechanism of the efficacy of huCD26mAb on human osteoclast (OC) development.

backbone and elicits ADCC and direct anti-tumor effects.[13,15] Our present work indicates that human OCs are intensely stained with CD26, but when human early OC differentiation is blocked by treating with huCD26mAb, CD26-stained multinuclear OCs are barely detected. A potential explanation for this finding may be that surface-expressed CD26 on human OCs are internalized by huCD26mAb and that CD26 expression is lost in multinuclear OCs.[18] The reduced level of CD26-stained OCs, with the resultant decline in CD26-mediated migration, might result in the decreased formation of mature human OCs. To identify the detailed mechanism of action by huCD26mAb on human OC development *in vitro*, we generated and purified huCD26mAb-F(ab′)$_2$ and investigated its effects on human OC formation. The present study clarified that huCD26mAb-F(ab′)$_2$ dose-dependently inhibits human OC differentiation via blockade of the p38 MAPK-mi/Mitf phosphorylation pathway, as does huCD26mAb. The inhibitory mechanism is therefore not dependent on the huCD26mAb-Fc domain. The p38 MAPK inhibitor also strongly blocks human OC differentiation by suppressing p38 MAPK phosphorylation and subsequent mi/Mitf activation in human OC precursor cells. These data suggest that the inhibitory mechanism of action during human early OC differentiation by huCD26mAb is caused by p38 MAPK dephosphorylation and mi/Mitf inactivation *in vitro*. Moreover, human OC functions are induced independent from CD26-p38MAPK mediated signaling. Although, DPPIV enzymatic activity is required for CD26-mediated T cell co-stimulation,[11] DPPIV activity in CD26 is not significantly correlated with human OC differentiation and maturation. Further studies will address the direct and indirect effects of huCD26mAb on tumor cells and bone stromal cells, including OCs in patients with osteolytic bone metastasis. To this end, the use of CD26 knockout mice will be important for examining not only the contribution of CD26 to normal skeletal physiology but also for answering questions pertaining to the function of CD26 in other human tissues.

Our findings have significant implications for the clinical care and novel therapeutic interventions of patients with osteolytic bone lesions following metastasis. Recently, several trials have demonstrated that anti-RANKL monoclonal antibody, denosumab, can significantly reduce SREs associated with osteolytic metastatic cancers such as breast cancer, as well as osteoblastic metastatic cancers such as prostate carcinoma.[45–48] The therapeutic intervention which targets the RANK pathway, thereby blocking OC differentiation, represents a novel strategy in the management of skeletal complications of metastatic bone disease.[45–48] The Src inhibitor, MMP inhibitor, and Cathepsin K inhibitor are alternate promising drugs for impairing OC fusion and maturation. Similarly, huCD26mAb is a fully human monoclonal antibody that regulates human OC differentiation by modulating the RANK signaling pathway and inactivating the downstream intracellular MKK3/6-p38 MAPK-mi/Mitf signaling pathway, thus blocking early OC differentiation. The effect of huCD26mAb is expected to reduce SREs and to thereby improve

Fig. 8. huCD26mAb does not directly affect functions of mature OCs. (*A*) Human OC culture was performed in the absence or presence of huCD26mAb (0, 0.1, 1.0, 10 μg/ml). huCD26mAb was added every 48 hours, for a total of 4 doses from day 0 (on day 0, 2, 4 and 6; protocol 1), from day 5 (on day 5, 7, 9 and 11; protocol 2), or from day 8 (on day 8, 10, 12 and 14; protocol 3) (see Materials and Methods). (*B*) The effect of huCD26mAb on calcium phophate substrate resorption activity in mature OCs. Calcium phosphate substrate resorption activity assay was performed in the absence or presence of huCD26mAb or huCD26mAb-F(ab′)$_2$, using protocol 1 or protocol 2. Microphotographs of OCs (black stained) on day 14 in a CaP-coated plate, demonstrating pit formation, are shown. Calcium phosphate substrate resorption activity was also evaluated by measuring the fluorescence intensity of the conditioned medium. (a) IgG control: multiple large pits are evident in the absence of huCD26mAb; (b) huCD26mAb 0.1 μg/ml (protocol 1); (c) huCD26mAb 1.0 μg/ml (protocol 1); (d) huCD26mAb 10 μg/ml (protocol 1); huCD26mAb treatment resulted in reduced numbers and sizes of pits in a dose-dependent manner. (e) negative control (without sRANKL); (f) huCD26mAb-F(ab′)$_2$ 10 μg/ml (protocol 1); (g) huCD26mAb 10μg/ml (protocol 2), (h) huCD26mAb-F(ab′)$_2$ 10μg/ml (protocol 2); The addition of huCD26mAb did not have significant inhibitory effect on human OC development. (a–h) original magnification: ×200. (*C*) and (*D*) The inhibitory effects of huCD26mAb (0, 0.1, 1.0, 10 μg/ml) or huCD26mAb-F(ab′)$_2$ (10 μg/ml) on OCs on the resorption of calcium phosphate-coated plates induced by RANKL. Calcium phosphate substrate resorptin activity was evaluated by (a) fluorescence intensity and (b) pit area. Antibodies were added, using protocol 1, protocol 2 or protocol 3. *Columns*, means plus minus SD; $n = 3$. $^*p < 0.05$, $^{**}p < 0.01$. (*E*, *F*) Changes in levels of secreted TRAP-5b and C-terminal cross-linked telopeptides of type 1 collagen (CTX) derived from OC supernatants were measured by enzyme-linked immunosorbent assay (ELISA) on day 7 of human OC culture, as described in Materials and Methods. Note the dose-dependent reduced levels of both TRAP-5b and CTX derived from OCs in the presence of huCD26mAb or huCD26mAb-F(ab′)$_2$, using protocol 1, whereas no reduction in the presence of huCD26mAb, using protocol 2, or protocol 3 was observed. *Columns*, means plus minus SD; $n = 3$. $^*p < 0.05$, $^{**}p < 0.01$. (*G*) In human OC culture, SB203580 (10, 20, 100 μM) had also significant inhibitory effect on TRAP-5b activity in a dose-dependent manner; however, SB203580 (100 μM) added, using protocol 2, did not have significant effects on mature OC formation. *Colums* represent mean plus or minus SD; $n = 3$. $^{**}p < 0.05$, $^*p < 0.01$.

the quality of life for patients with osteolytic bone lesions following metastasis.

Our previous data indicated that huCD26mAb represents an effective therapeutic tool for treating tumors, including CD26-positive malignant lymphoma. huCD26mAb inhibits tumor cell growth by regulating p38 MAPK phosphorylation.[14,15] Previous studies on CD26 yielded various results in several cancers, suggesting that the effect of CD26 on the growth and metastatic potential of various tumors may be dependent on the type of cancer.[14,15] Preclinical studies have shown that the inhibition of CD26 in malignant mesothelioma suppressed tumor growth and invasiveness.[13,18,20] In addition, it has been reported that CD26+ cells are capable of initiating growth of metastasis in distant organs and CD26 plays a functional role in the invasive capacity of the CD26-positive CSCs in colorectal cancer.[23] CD26-positive cells in the primary colorectal cancer are associated with early metastatic relapse after systemic chemotherapy, probably due to the failure of chemotherapy to eradicate CSCs.[23] Therefore, targeting these CSCs with huCD26mAb may also be a novel therapeutic strategy.

Bone disease in MM is caused by the disruption of the delicate balance between OB-mediated bone formation and OC-mediated bone resorption. CD26 expression can be detected slightly in MM cells (data not shown) but intensely in MM-derived activated OCs. The proliferation and survival of MM cells requires the interplay between MM cells in the bone marrow and the microenvironment, including activated OCs. MM cells express vessel endothelial growth factor (VEGF), which acts as an alternative to M-CSF. MM cells also interact with OCs and secrete MIP-1 and RANKL, thus further activating the surrounding OCs and leading to extended bone destruction.[4,8,9] Activated OCs also produce IL-6, which is essential for the proliferation of MM cells.[8,9] Thus, the blockade of CD26 by huCD26mAb is expected to impair not only functional OC development and activation, but also the interplay between activated OCs and MM cells. Therefore, targeting the interplay between MM cells and OCs holds the potential for improving long-term disease control and prolonging MM patient survival.

In conclusion, we demonstrated the importance of CD26 expression in normal human OCs. M-CSF and RANKL induced human OC differentiation, in association with CD26 expression in monocyte-macrophage lineage cells and OC precursor cells. CD26 expression induces MKK3/6-p38 MAPK-mi/Mitf phosphorylation in human OC precursor cells. Furthermore, it was suggested that huCD26mAb blocks OC precursor differentiation into OCs *in vitro* during the early phase of human OC development, via the blockade of MKK3/6-p38 MAPK-mi/Mitf phosphorylation and the subsequent impairment of mature OC functions. Further analysis of CD26 functions and RANK-dependent p38 MAPK will also support the notion that the blockade of the CD26 cascade of the RANK signaling pathway with huCD26mAb impairs the development of human OCs and may become a promising alternative therapeutic strategy for osteolytic bone lesions following metastasis including MM to reduce the occurrence of SREs.

Disclosures

TY reports being a consultant for Y's Therapeutics and Kissei Pharmaceutical Ltd. All other authors state that they have no conflicts of interest.

Acknowledgments

We would like to express thanks to Dr. N. Kiyokawa at the National Center for Child Health and Development, Tokyo, Japan, and Dr. K. Ohnuma at the Institute of Medical Science, the University of Tokyo, Tokyo, Japan for providing us with antibodies. We also thank Dr. K. Emoto at Keio University, School of Medicine, Tokyo, Japan, for his helpful advice regarding pathology. This work was supported by Grants-in-Aid for Scientific Research from the Ministry of Education in Japan (H.N. 25430157, T.Y. 20590354, M.S. 1770124), the Program for Promotion of Fundamental Studies in Health Sciences of the National Institute of Biomedical Innovation (T.Y. and C.M. 07-17), and a Grant-in-Aid for Drug Design Biomarker Research (T.Y. and C.M., H24-B10-003) from the Ministry of Health, Labor and Welfare, Japan.

Authors' roles: HN designed the research studies, performed all the experiments, analyzed the data and wrote the manuscript; HS and HM assisted with the immunohistochemical staining experiments; MH, CM, and MS contributed to the coordination of experiments. TY directed the project and contributed to the experimental design, data interpretation, and writing of the manuscript. All authors reviewed and gave final approval for the paper.

References

1. Boyle WJ, Simonet WS, Lacey DL. Osteoclast differentiation and activation. Nature. 2003;423(6937):337–42.
2. Matsuo K, Irie N. Osteoclast-osteoblast communication. Arch Biochem Biopys. 2008;473(2):201–9.
3. Miyamoto T, Arai F, Ohneda O, Takagi K, Anderson DM, Suda T. An adherent condition is required for formation of multinuclear osteoclasts in the presence of macrophage colony-stimulating factor and receptor activator of nuclear factorκB ligand. Blood. 2000;96 (13):4335–43.
4. Udagawa N, Takahashi N, Jimi E, et al. Osteoblasts/stromal cells stimulate osteoclast activation through expression of osteoclast differentiation factor/RANKL but not macrophage colony-stimulating factor. Bone. 1999;25(5):517–23.
5. Nakshima T, Hayashi M, Fukunaga T, et al. Evidence of osteocyte regulation of bone homeostasis through RANKL expression. Nat Med. 2011;17(10):1231–34.
6. Xiong J, Onal M, Jilka RL, Weinstein RS, Manolagas SC, O'Brien CA. Matrix-embedded cells control osteoclast formation. Nat Med. 2011; 17(10):1235–41.
7. Giuliani N, Colla S, Rizzoli V. New insight in the mechanism of osteoclast activation and formation in multiple myeloma: Focus on the receptor activator of NFκB ligand (RANKL). Exp Hematol. 2004; 32(8):685–91.
8. Yaccobi S, Wezeman MJ, Henderson A, et al. Cancer and the microenvironment: myeloma-osteoclast interactions as a model. Cancer Res. 2004;64(6):2016–23.
9. Dougall WC. Molecular pathways: Osteoclast-dependent and osteoclast-independent roles of the RANKL/RANK/OPG pathway in tumorigenesis and metastasis. Clin Cancer Res. 2012;18(2): 326–35.
10. Eghabli FG, Khosla S, Sanyal A, Boyle WJ, Lacey DL, Riggs BL. Role of RANK ligand in mediating increased bone resorption in early menopausal woman. J Clin Invest. 2003;111(8):1221–30.
11. Dong RP, Tachibana K, Hegen M, Scharpe S, Schlossman SF, Morimoto C. Correlation of the epitopes defined anti-CD26mAbs and CD26 function. Mol Immunol. 1998;35(1):13–21.
12. Kobayashi S, Ohnuma K, Uchiyama M, et al. Association of CD26 with CD45RA outside lipids rafts attenuates cord blood T-cell activation. Blood. 2004;103(3):1002–10.

13. Inamoto T, Yamada T, Ohnuma K, et al. Humanized anti-CD26 monoclonal antibody as a treatment for malignant mesothelioma tumors. Clin Cancer Res. 2007;13(14):4191–200.
14. Sato T, Yamochi T, Yamochi T, et al. CD26 regulates p38 mitogen-activated protein kinase-dependent phosphorylation of Integrin β1, adhesion to extracellular matrix, tumorgenicity, of T-anaplastic large cell lymphoma. Karpas 299. Cancer Res. 2005; 65(15):6950–6.
15. Yamochi T, Yamochi T, Aytac U, et al. Regulation of p38 phosphorylation and topoisomerase IIαexpression in the B-cell lymphoma Jiyoye by CD26/dipeptidyl peptidase IV is associated with enhanced in vitro and in vivo sensitivity to doxorubicin. Cancer Res. 2005;65(5):1973–83.
16. Dang NH, Torimoto Y, Sugita K, et al. Cell surface modulation of CD26 by anti-1F7 monoclonal antibody. Analysis of surface expression on T cell activation. J Immunol. 1990;145(12):3963–71.
17. Inamoto T, Yamochi T, Ohnuma K, et al. Anti-CD26 monoclonal antibody mediated G1-S arrest of human renal cell carcinoma Caki-2 is associated with retinoblastoma substrate dephosphorylation, cyclin dependent kinase 2 reduction, p27kip1 enhancement, and distribution of binding to the extracellular matrix. Clin Cancer Res. 2006;12(11):3470–7.
18. Aoe K, Amataya VJ, Fujimoto N, et al. CD26 overexpression is associated with prolonged survival and enhanced chemosensitivity in malignant pleural mesothelioma. Clin Cancer Res. 2012;18 (5):1447–56.
19. Kameoka J, Ichinohasama R, Inoue H, et al. CD26, together with cell surface adenosine deaminase, is selectively expressed on ALK-positive, but not on ALK-negative, anaplastic large cell lymphoma and Hodgkin's lymphoma. Leuk Lymph. 2006;47(10): 2181–8.
20. Amataya VJ, Takeshima Y. Kushitani, Yamada T, Morimoto C, Inai K, Overexpression of CD26/DPPIV in mesothelioma tissue and mesothelioma cell lines. Oncology Reports. 2011;26(6):1369–75.
21. Hirai K, Kotani T, Aratake Y, Ohtaki S, Kuma K. Dipeptidyl peptidase IV (DPPIV/CD26) staining predicts distant metastasis of ' benign' thyroid tumor. Pathol Int. 1999;49(3):264–5.
22. Yamaguchi U, Nakayama R, Honda K, et al. Distant gene expression-defined classes of gastrointestinal stromal tumor. J Clin Oncol. 2008;26(25):4100–8.
23. Pang R, Law WL, Chu AC, et al. A subpopulation of CD26+ cancer stem cells with metastatic capacity in human colorectal cancer. Cell Stem Cell. 2010;6(6):603–15.
24. Fujita K, Iwasaki M, Ochi H, et al. Vitamin E decreases bone mass by stimulating osteoclast fusion. Nat Med. 2012;18(4):589–94.
25. Ashley JW, Shi Z, Zhao H, Li X, Kesterson RA, Feng X. Genetic Ablation of CD68 results in mice with increased bone and dysfunctional osteoclasts. PloS One. 2011;6(10):e25838.
26. Leung R, Cuddy K, Wang Y, Rommens J, Glogaue M. Sbds is required for Rac2-mediated monocytes migration and signaling downstream of RANK during osteoclastgenesis. Blood. 2011;117(6):2044–53.
27. Levaot N, Simoncic PD, Dimitriou LD, et al. 3BP-deficient mice are osteoporotic with impaired osteoblast and osteoclast functions. J Clin Invest. 2011;121(8):3244–57.
28. Irie N, Takeda Y, Watanabe Y, et al. Bidirectional signaling through EphrinA2-EphA2 enhances osteoclastgenesis and suppresses osteoclastgenesis. J Biol Chem. 2009;284(21):14637–44.
29. Pennisi A, Li X, Ling W, et al. Inhibitor of DASH protease affects expression of adhesion molecules in osteoclast and reduces myeloma growth and bone disease. Br J Haematol. 2009;145(6): 775–87.
30. Kim K, Lee SH, Ha Kim J, Choi Y, Kim N. NFATc1 induces osteoclast fusion via up-regulation of Atp6v0d2 and the dendritic cell specific transmembrane protein (DC-STAMP). Mol Endocrinol. 2008;22(1): 176–85.
31. Song I, Kim JH, Kim K, Jin HM, Youn BU, Kim N. Regulatory mechanism of NFATc1 in RANKL-induced osteoclast activation. FEBS Letters. 2009;583(14):2435–40.
32. Li X, Udagawa N, Itoh K, et al. p38MAPK-mediated signals are required for inducing osteoclast differentiation but not for osteoclast function. Endocrinol. 2002;143(8):3105–13.
33. Matsumoto M, Sudo T, Saito T, Osada H, Tsujimoto M. Involvement of p38 mitogen-activated protein kinase signalling pathway in osteoclastgenesis mediated by receptor activator of NF-κB ligand (RANKL). J Biol Chem. 2000;275(40):31155–61.
34. Mansky KC, Sankar U, Han J, Ostrowski MC. Microthalmia transcription factor is a target for the p38 MAPK pathway on response to receptor actovator of NF-κB ligand signaling. J Biol Chem. 2002;277 (13):11077–83.
35. Miyazaki T, Miyauchi S, Anada T, Imaizumi H, Suzuki O. Evaluation of osteoclaststic activity using calcium phosphate coating combined with labeled polyanion. Anal Biochem. 2011;410(1): 7–12.
36. Rissanen JP, Suominen MI, Peng Z, et al. Secreted tartrate-resistant acid phosphates 5b is a marker of osteoclast number in human osteoclast cultures and the rat ovariectomy model. Calcif Tissue Int. 2008;82(2):108–115.
37. Raingeaud J, Gupta S, Rogers JS, et al. Pro-inflammatory cytokines and environmental stress cause p38 mitogen-activated protein kinase activation by dual phosphorylation on throsine and threonine. J Biol Chem. 1995;270(13):7420–26.
38. Li X, Udagawa N, Takami M, Sato N, Kobayashi Y, Takahashi N. p38 mitogen-activated protein kinase is crucially involved in osteoclast differentiation but not in cytokine production, phagocytosis, or dendritic cell differentiation of bone marrow macrophages. Endocrinol. 2003;144(11):4999–5005.
39. Zwerina J, Hayer S, Redlich K, et al. Activation of p38 MAPK is a key step in tumor necrosis factor-mediated inflammatory bone destruction. Arth Rheum. 2006;54(2):463–72.
40. Bohm C, Hayer S, Kilian A, et al. The α-isoform of p38 MAPK specifically regulates arthritic bone loss. J Immunol. 2009;183:5938–47.
41. Voso MT, Pantel G, Rutella S, et al. Rituximab reduces the number of peripheral blood B-cells in vitro mainly by effector cell-mediated mechanisms. Hematologica. 2002;87(9):918–25.
42. Clynes RA, Towers TL, Presta LG, Avetch JV. Inhibitory Fc receptors modulate in vivo cytotoxicity against tumor targets. Nat Med. 2000;6 (4):443–6.
43. Cartron G, Dacheux L, Salles G, et al. Therapeutic activity of humanized anti-CD20 monoclonal antibody and polymorphism in IgG Fc receptor FcgammaRIIIa gene. Blood. 2002;99(3):754–8.
44. Ishida T, Ueda R. Antibody therapy for Adult T-cell leukemia-lymphoma. Int J Hematol. 2011;94(5):443–452.
45. Stopeck AT, Lipton A, Body JJ, et al. Denosumab compared with zoledronic acid for the treatment of bone metastasis in patients with advanced breast cancer: a randomized double-blind study. J Clin Oncol. 2010;28(35):5132–9.
46. Fizazi K, Carducci M, Smith M, et al. Denosumab versus zoledronic acid for the treatment of bone metastasis in men with castration-resistant prostate cancer:randomized, double-blind study. Lancet. 2011;377(9768):813–22.
47. Henry DH, Costa L, Goldwasser F, et al. Randomized double-blind study of denosumab versus zoledronic acid in the treatment of bone metastasis in patients with advanced cancer excluding breast and prostate cancer or multiple myeloma. J Clin Oncol. 2011;29 (9):1125–32.
48. Castellano D, Sepulveda JM, Garcia-Escobar I, Rodriguez-Antonin A, Cortes-Funes H. The role of RANKL ligand inhibition in cancer: the story of denosumab. Oncol. 2011;16(2):136–45.

Biochemical and Biophysical Research Communications 447 (2014) 609–615

Contents lists available at ScienceDirect

Biochemical and Biophysical Research Communications

journal homepage: www.elsevier.com/locate/ybbrc

CD26-mediated regulation of periostin expression contributes to migration and invasion of malignant pleural mesothelioma cells

Eriko Komiya [a], Kei Ohnuma [a,*], Hiroto Yamazaki [a], Ryo Hatano [a], Satoshi Iwata [a], Toshihiro Okamoto [a], Nam H. Dang [b], Taketo Yamada [c], Chikao Morimoto [a]

[a] Department of Therapy Development and Innovation for Immune Disorders and Cancers, Graduate School of Medicine, Juntendo University, 2-1-1, Hongo, Bunkyo-ku, Tokyo 113-8421, Japan
[b] Division of Hematology/Oncology, University of Florida, 1600 SW Archer Road, Box 100278, Room MSB M410A, Gainesville, FL 32610, USA
[c] Department of Pathology, Keio University School of Medicine, 35 Shinanomachi, Shinjuku-ku, Tokyo 160-8582, Japan

ARTICLE INFO

Article history:
Received 1 April 2014
Available online 18 April 2014

Keywords:
Malignant pleural mesothelioma
Periostin
CD26
Src
Twist1

ABSTRACT

Malignant pleural mesothelioma (MPM) is an aggressive malignancy arising from mesothelial lining of pleura. It is generally associated with a history of asbestos exposure and has a very poor prognosis, partly due to the lack of a precise understanding of the molecular mechanisms associated with its malignant behavior. In the present study, we expanded on our previous studies on the enhanced motility and increased CD26 expression in MPM cells, with a particular focus on integrin adhesion molecules. We found that expression of CD26 upregulates periostin secretion by MPM cells, leading to enhanced MPM cell migratory and invasive activity. Moreover, we showed that upregulation of periostin expression results from the nuclear translocation of the basic helix-loop-helix transcription factor Twist1, a process that is mediated by CD26-associated activation of Src phosphorylation. While providing new and profound insights into the molecular mechanisms involved in MPM biology, these findings may also lead to the development of novel therapeutic strategies for MPM.

© 2014 Elsevier Inc. All rights reserved.

1. Introduction

Malignant pleural mesothelioma (MPM) is an aggressive malignancy arising from mesothelial lining of pleura [1]. It is generally associated with a history of asbestos exposure and has a very poor prognosis [2]. Once rare, the incident of MPM has increased in industrialized nations as a result of past wide spread exposure to asbestos [1,2]. The incident is predicted to increase further in the next decades, especially in developing countries where asbestos has not yet been prohibited [2]. Due to the lack of efficacy of conventional treatments, novel therapeutic strategies are urgently needed to improve outcomes [3].

CD26 is a 110-kDa type II transmembrane glycoprotein with known dipeptidyl peptidase IV (DPPIV, EC 3.4.14.5) activity in its extracellular domain and is capable of cleaving N-terminal dipeptides with either L-proline or L-alanine at the penultimate position [4]. CD26 has an important role in T cell biology and overall immune function [5]. In addition, CD26 is expressed in various cancers and is involved in cancer biology [6]. CD26 itself appears to be a novel therapeutic target, and anti-CD26 monoclonal antibody (mAb) treatment resulted in both *in vitro* and *in vivo* anti-tumor activity against several tumor types, including lymphoma and renal cell carcinoma [7–9]. Of note is that CD26 expression is associated with both pro- or anti-tumor effects in different cancers [6].

Recently, we showed that mesothelioma cells expressing high level of CD26 displayed high proliferative activity and invasiveness, and microarray analysis of CD26 knockdown and CD26-transfected mesothelioma cells showed that CD26 expression was closely linked to expression of genes contributing to cell proliferation and cell cycle regulation [10]. More recently, we demonstrated that CD9 suppressed cell adhesion by inhibiting CD26–α5β1 integrin complex through its negative regulation of

Abbreviations: bHLH, basic helix-loop-helix; csh, control shRNA; csi, control siRNA; FAS1, fasciclin I; CD26/10Chi, stable transfectant of MPM cell line, MSTO-211H with CD26–CD10 chimeric receptor; CD26WT, stable transfectant of MPM cell line, MSTO-211H with a full-length CD26; DPPIV, dipeptidyl peptidase IV; ECM, extracellular matrix; ELISA, enzyme-linked immunosorbent assay; EMT, epithelial–mesenchymal transition; mAb, monoclonal antibody; MPM, malignant pleural mesothelioma; MSTO-P, MPM cell line MSTO-211H parental cells; pAb, polyclonal antibody; qPCR, quantitative real-time RT-PCR; shRNA, short hairpin RNA; siRNA, small interference RNA; TBP, TATA binding protein.

* Corresponding author. Fax: +81 3 3868 2310.
E-mail address: kohnuma@juntendo.ac.jp (K. Ohnuma).

http://dx.doi.org/10.1016/j.bbrc.2014.04.037
0006-291X/© 2014 Elsevier Inc. All rights reserved.

CD26 [11]. These observations suggest that CD26 regulates the interaction of MPM cells with the extracellular matrix (ECM) via yet-to-be-determined integrin adhesion molecules. Meanwhile, with proximal signaling events associated with the cytoplasmic 6 amino acid residues of CD26 being characterized in normal human T lymphocytes [12], it is conceivable that similar CD26-mediated proximal signaling events, which remain to be clarified, play a pivotal role in MPM cell motility.

In the current study, we extended our previous studies on the enhanced motility and increased CD26 expression level in MPM cells to demonstrate CD26 upregulates expression and secretion of periostin (or osteoblast-specific factor 2) by MPM cells, leading to augmented migratory and invasive activity of MPM cells. Moreover, we showed that upregulation of periostin resulted from nuclear translocation of Twist1, a basic helix-loop-helix (bHLH) transcription factor, via CD26-associated phosphorylation of Src.

2. Materials and methods

2.1. Cell lines, antibodies and reagents

The human MPM cell line MSTO-211H (MSTO-P) was obtained from the American Type Culture Collection. JMN cells were a kind gift from Dr. Brenda Gerwin (Laboratory of Human Carcinogenesis, National Institutes of Health, Bethesda, MD, USA). MSTO-P were stably transfected with a full-length CD26 (CD26WT), CD26–CD10 chimeric receptor (CD26/10Chi) or vector alone (MSTO-Mock), which were developed in our laboratory [13]. Anti-CD26 goat polyclonal antibody (pAb) (AF1180) was from R&D Systems (USA), anti-Src kinase rabbit monoclonal antibody Ab (mAb) (36D10) and anti-phospho-Src family (Tyr416) (p-Src) rabbit mAb (D49G4) were from Cell Signaling Technology (USA), anti-Twist mouse mAb (Twist2C1a) and anti-TATA binding protein (TBP) mouse mAb (mAbcam 51841) from Abcam (UK), and anti-β-actin mouse mAb (AC-74) from Sigma–Aldrich (USA). Src specific inhibitor (PP2) was from Merk Millipore (USA) and stocked in 10 mM with DMSO. Measurement of periostin in supernatants was performed using commercially available enzyme-linked immunosorbent assay (ELISA) kit (Aviscera Bioscience, USA). The supernatants were harvested for measurement 48 h after (1×10^5/ml of each cell type were plated in the culture dish.

2.2. Short hairpin RNA (shRNA) and small interference RNA (siRNA)

To deplete endogenous CD26, two shRNAs were used (reference sequence: NM_001935) [14]. To deplete endogenous periostin, two siRNAs were used (reference sequence: NM_006475). The sequences of CD26-shRNAs and periostin-siRNAs are shown in Supplementary Table S1. shRNA and siRNA were obtained from Sigma–Aldrich. Knockdown experiments in MPM cell lines using shRNA or siRNA were achieved as described previously [11].

2.3. Cell migration and invasion assays

For cell migration assay, cells (500 μl of 1×10^5/ml in 0.1% FBS-RPMI1640) were seeded onto uncoated filters in a 24-well Transwell chamber (8-μm pore size; Costar, USA) with 750 μl of indicated medium in the lower cell, and allowed to migrate at 37 °C in 100% humidifier. For cell invasion assay, cells (500 μl of 1×10^5/ml in 0.1% FBS-RPMI1640) were seeded onto filters of a 24-well Transwell chamber that were coated with Matrigel (BD Biosciences, USA) with 750 μl of indicated medium in the lower cell. Migration or invasion of the cells through the chamber to the underside of the filter was assessed as described previously [11].

2.4. Western blotting and lipid raft fractioning

Total cell lysates, cytosolic and nuclear extracts for Western blot analysis were prepared as described elsewhere [15]. To obtain the lipid raft membrane fraction, indicated cell types (each, 1×10^8) were lysed on ice with 1 ml 1% Triton X-100 and 1 mM PMSF in MNE buffer (25 mM MES [pH 6.5], 150 mM NaCl, 5 mM EDTA), followed by sucrose-gradient ultracentrifugation as described previously [16]. Samples were submitted to sodium dodecyl sulfate–polyacrylamide gel electrophoresis (SDS–PAGE) under reducing conditions and Western blot analysis using the indicated specific antibodies.

2.5. Quantitative real-time RT-PCR (qPCR) assay

In experiments assessing expression of mRNA of MPM cells, extraction of total RNA, generation of mRNA and quantification of mRNA were performed as described previously [17]. Expression levels of mRNA were calculated on the basis of standard curves generated for each gene and hypoxanthine phosphoribosyltransferase 1 (HPRT1) mRNA was used as an invariant endogenous control. Sequences of primers used in qPCR analysis are shown in Supplementary Table S2.

2.6. Statistical analysis

All experiments were performed in triplicates and repeated at least 3 times. Data were expressed as mean values ± SEM (standard error of the mean) and analyzed by one-way or two-way ANOVA followed by the Tukey–Kramer *post-hoc* test. The level of significance was $P < 0.05$. The calculations were conducted using Prism6.0 software (GraphPad Software, USA).

3. Results

3.1. Upregulation of periostin in CD26-expressing MPM cells

To understand the nature of CD26 association with certain molecules and MPM biology, we previously performed microarray analysis of CD26-depleted and CD26 over-expressed mesothelioma cells, with data having been deposited in NCBI's Gene Expression Omnibus and being accessible through GEO Series accession number GSE52216 [11]. Among these, we focused in the present study on the upregulation of the secretory protein periostin in CD26-expressing MPM cells as being correlated with migratory and invasive activity as integrin adhesion molecules. To determine that CD26 expression is associated with periostin upregulation, we first conducted knockdown experiments using shRNA against CD26 in JMN cells, which express CD26 endogenously. Expression of CD26 was determined by flow cytometry of JMN in the presence of control shRNA (csh) or two different sequences of CD26-shRNAs (sh-1 or sh-2) (Supplementary Fig. S1A). As shown in Fig. 1A, a significant decrease in the level of periostin mRNA was observed in JMN cells in the presence of CD26-shRNAs. In addition, periostin concentration in culture supernatant was significantly decreased in CD26-knockdown JMN cells (Fig. 1B). These data indicate that CD26 and periostin are correlatively expressed in MPM cells.

We next define the crucial role of the CD26 cytoplasmic region in regulating periostin expression. For this purpose, we analyzed periostin expression in MSTO-CD26WT, MSTO-CD26/10Chi and MSTO-Mock cells. The CD26–CD10 chimeric receptor (CD26/10Chi) was composed of the N-terminal cytoplasmic region of human CD10 (1–23 amino acid position) ligated to the transmembrane and extracellular regions of human CD26 (7–766 amino acid position), and this mutant chimeric receptor was shown to

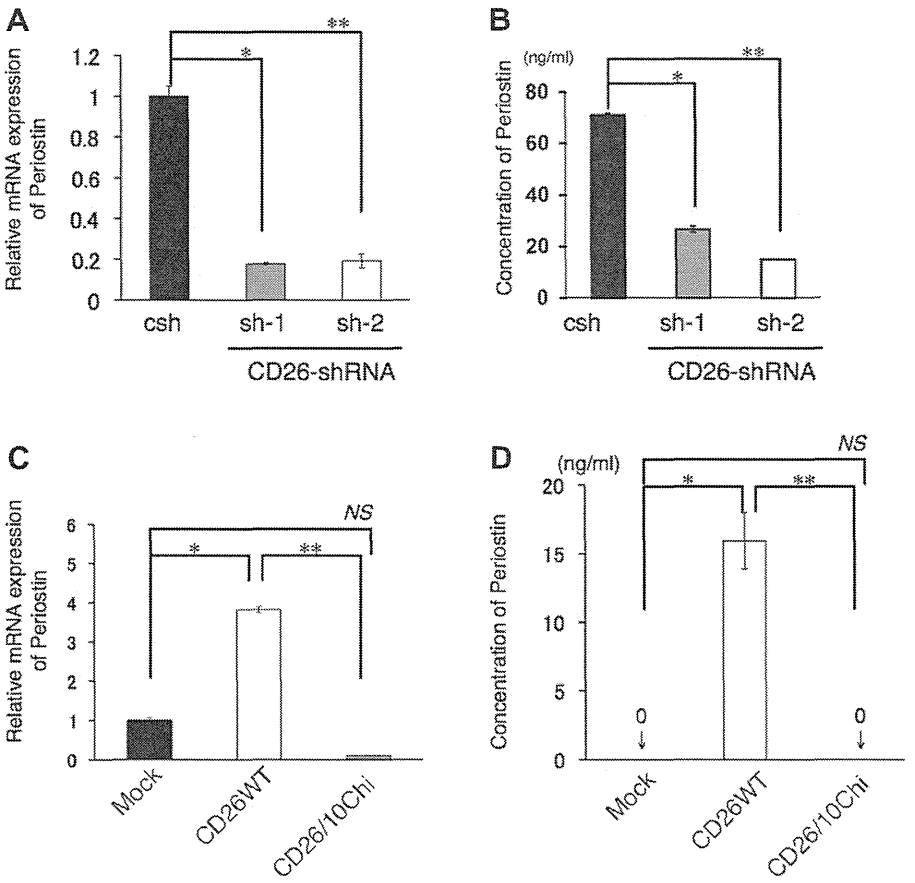

Fig. 1. Upregulation of periostin in CD26-expressing MPM cells. (A) JMN cells were transfected with two different CD26-shRNAs (sh-1 or sh-2) or control shRNA (csh), and mRNA expression of periostin was quantified by real-time RT-PCR. Each expression was normalized to hypoxanthine phosphoribosyltransferase 1 (HPRT1) and relative expression levels compared with the sample of JMN with csh were shown. Data are shown as mean ± SEM of three different experiments. *, **$P < 0.0001$. (B) Production of periostin protein in the culture supernatants of shRNA-transfected JMN (csh. sh-1 or sh-2) was quantified by ELISA. Data are shown as mean ± SEM of three different experiments with triplicates. *, **$P < 0.0001$. (C) In MSTO-Mock, MSTO-CD26WT or MSTO-CD26/10Chi cells, mRNA expression of periostin was quantified by real-time RT-PCR. Each expression was normalized to HPRT1 and relative expression levels compared with the sample of MSTO-Mock were shown. Data are shown as mean ± SEM of three different experiments. *, **$P < 0.0001$. *NS* denotes 'not significant'. (D) Production of periostin protein in the culture supernatants of MSTO-Mock, MSTO-CD26WT or MSTO-CD26/10Chi cells was quantified by ELISA. Data are shown as mean ± SEM of three different experiments with triplicates. *, **$P < 0.0001$. *NS* denotes 'not significant'.

abrogate CD26-mediated costimulation in T cells [18]. CD10, as is the case with CD26, is a type II transmembrane glycoprotein with a relatively short cytoplasmic tail containing signal sequence that has an expected membrane topology similar to CD26 [19,20]. Cell surface CD26 expression levels were confirmed by flow cytometry (Supplementary Fig. S1B). As shown in Fig. 1C, periostin mRNA level was significantly increased in MSTO-CD26WT, compared to MSTO-CD26/10Chi or MSTO-Mock. In addition, using ELISA, we observed that protein expression level of periostin was significantly increased in MSTO-CD26WT, compared to MSTO-CD26/10Chi or MSTO-Mock (Fig. 1D). These observations indicate that periostin upregulation is associated with expression of a full-length CD26 molecule, but not with the CD26 extracellular region containing DPPIV activity, suggesting that the intracytoplasmic region of CD26 mediates upregulation of periostin in MPM cells.

3.2. CD26 expression leads to nuclear translocation of Twist1 via activation of Src

It has been previously shown that transcription of periostin is regulated by the bHLH transcription factor Twist1 as a downstream signaling event of c-Src [21,22]. For this purpose, we analyzed the expression levels of these signaling molecules in JMN cells in the presence of CD26-shRNAs. As shown in Fig. 2A, a significant decrease in p-Src level was observed in JMN cells in the presence of CD26-shRNAs (lanes 2 and 3), compared to those treated with control shRNA (lane 1). In addition, as shown in Fig. 2B, p-Src level was increased in MSTO-CD26WT (lane 2), compared to MSTO-Mock (lane 1) or MSTO-CD26/10Chi (lane 3). Moreover, as shown in Fig. 2C, a significant decrease in nuclear Twist1 level was observed in JMN cells in the presence of CD26-shRNAs (lanes 2 and 3 of second panel from the bottom), compared to those treated with control shRNA (lane 1 of second panel from the bottom). Furthermore, as shown in Fig. 2D, nuclear Twist1 level was clearly increased in MSTO-CD26WT (lane 2), compared to MSTO-Mock (lane 1) or MSTO-CD26/10Chi (lane 3), with Twist1 level being higher in the cytoplasmic fraction (top panel) than in the nuclear fraction (second panel from the bottom). These data suggest that the expression of CD26, particularly its intracytoplasmic region, mediates increased Twist1 level and activity through phosphorylation of Src, resulting in enhanced periostin expression.

Since the cytoplasmic tail of CD26 consists of only 6 amino acids in length without any conserved kinase or protein-binding domain, it is unlikely that such a short cytoplasmic domain proximal to the membrane interacts directly with Src. On the other hand, lipid raft clustering plays a crucial role in CD26-mediated costimulatory signaling or activation of Src kinase [16,18,23]. We thus analyzed the molecular clustering induced by lipid raft aggregation in MPM cells. As shown in Fig. 2E, increased levels of CD26, p-Src and total Src molecules in lipid raft fractions were observed in

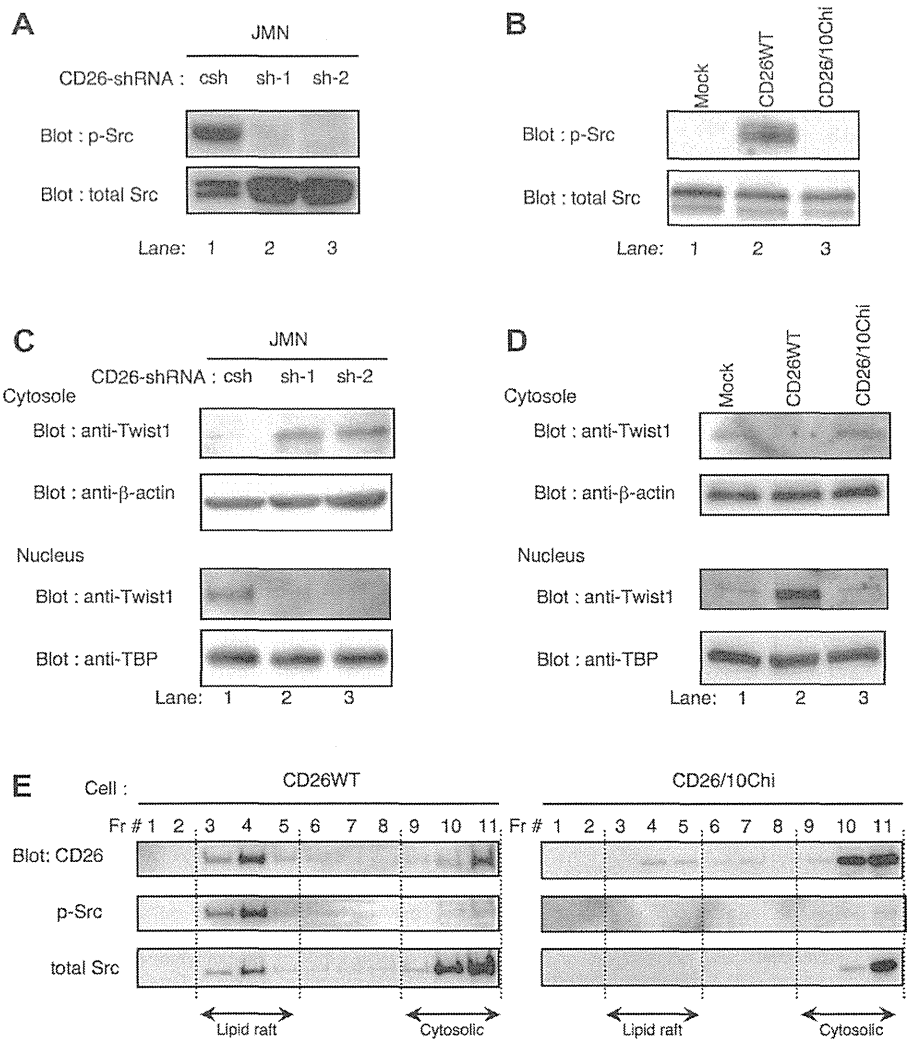

Fig. 2. Nuclear translocation of Twist1 via phosphorylation of Src. (A) Total lysates (each, 10 μg) from JMN transfected with two different CD26-shRNAs (sh-1 or sh-2) or control shRNA (csh) and immunoblotted using anti-phospho Src (p-Src) mAb followed by stripping and reprobing with anti-Src mAb (total Src). Similar results were obtained in three independent experiments. (B) Total lysates from each cell type were resolved by SDS–PAGE, and immnoblotted by the same method as conducted in (A). Similar results were obtained in three independent experiments. (C) Cytosolic (upper two panels) and nuclear extracts (lower two panels) (each, 10 μg) from JMN transfected with two different CD26-shRNAs (sh-1 or sh-2) or control shRNA (csh) were resolved by SDS–PAGE, and immnoblotted using anti-Twist1 mAb, followed by stripping and reprobing with anti-β-actin mAb or anti-TBP (TATA-binding protein) mAb, which were used as a quality control marker indicating equal amounts in the experiments. Similar results were obtained in three independent experiments. (D) Cytosolic (upper two panels) and nuclear extracts (lower two panels) from each cell type were resolved by SDS–PAGE, and immnoblotted by the same method as conducted in (C). Similar results were obtained in three independent experiments. (E) Lipid raft or cytosolic fractions of MSTO-CD26WT (left panels) or CD26/10Chi (right panels) cells were prepared by sucrose gradient ultracentrifugation. The distribution of CD26, phosphorylated Src (p-Src), and total Src was determined by immunoblotting with respective antibodies. Fraction number (Fr#) 3–5 or 9–11 contains lipid raft or cytosolic fractions, respectively. Similar results were obtained in three independent experiments.

MSTO-CD26WT (left panels), while in MSTO-CD26/10Chi, most CD26/10Chi and Src molecules were located in the cytosolic fractions, and phosphorylated Src was not observed (right panels). These results suggest that the cytoplasmic region of CD26 plays a pivotal role in the clustering of Src molecules in lipid rafts, hence providing a platform for downstream signaling leading to nuclear translocation of Twist1 in CD26-expressing MPM cells.

3.3. Src inhibitor decreases production of periostin

As shown above, since Src kinase appears to play an important role in the upregulation of periostin expression, we next examined whether this process is affected by Src inhibition. As shown in Fig. 3A, in the presence of the Src inhibitor PP2 (lane 2 of panels a or b), Twist1 nuclear translocation (second panels from the bottom) was clearly decreased in JMN or MSTO-CD26WT, compared to treatment with control solvent (lane 1 of panels a or b). Moreover, a significant decrease in periostin mRNA expression in JMN or MSTO-CD26WT treated with PP2 was observed (Fig. 3B). Similarly, a significant decrease in secretion of periostin in JMN or MSTO-CD26WT treated with PP2 was observed (Fig. 3C). These observations strongly suggest that expression of a full-length CD26 in MPM cells activates Src/Twist signaling, promoting subsequent upregulation of periostin expression and secretion.

3.4. Periostin enhances migration and invasion of MPM cells

We recently demonstrated that CD26–α5β1 integrin complex enhances cell migration and invasion in CD26-expressing MPM cells [11]. Since periostin plays a pivotal role in cell migration and invasion via its interaction with integrin and ECM [24], we next examined whether periostin enhances cell motility in MPM cells. As shown in Fig. 4A, a significant increase in migration or invasion was observed in MSTO-CD26WT (white bars of panels a